Fall 1994

Adaptive receivers for direct-spread and multi-carrier code division multiple access systems

Xiangqun Liu
New Jersey Institute of Technology

Copyright Warning & Restrictions

The copyright law of the United States (Title 17, United States Code) governs the making of photocopies or other reproductions of copyrighted material.

Under certain conditions specified in the law, libraries and archives are authorized to furnish a photocopy or other reproduction. One of these specified conditions is that the photocopy or reproduction is not to be "used for any purpose other than private study, scholarship, or research." If a, user makes a request for, or later uses, a photocopy or reproduction for purposes in excess of "fair use" that user may be liable for copyright infringement,

This institution reserves the right to refuse to accept a copying order if, in its judgment, fulfillment of the order would involve violation of copyright law.

Please Note: The author retains the copyright while the New Jersey Institute of Technology reserves the right to distribute this thesis or dissertation

Printing note: If you do not wish to print this page, then select "Pages from: first page # to: last page #" on the print dialog screen

ABSTRACT

ADAPTIVE RECEIVER FOR DIRECT-SPREAD AND MULTI-CARRIER CODE DIVISION MULTIPLE ACCESS SYSTEM

by
Xiangqun Liu

In this thesis, the detection of Direct Sequence Code Division Multiple Access (DS-CDMA) signals in an AWGN channel and Multi-Carrier (MC) CDMA signals in a time-dispersion channel is discussed.

The DS-CDMA receiver employs an adaptive multiuser interference canceler that utilizes deadzone limiters in the tentative decision stage. With weights adjusted adaptively, the prior knowledge of signal powers is unnecessary. The steady state error performance of this receiver is obtained and found to be superior to the performance of the same receiver using hard limiters for tentative decisions. The channel is considered non-fading in this receiver.

Modeling the frequency selective channel fading as narrowband flat-flat fading centered at each subcarrier, the MC-CDMA technique reduces the effect of channel dispersion. A decorrelating multiuser interference canceler is introduced in the MC-CDMA receiver to reduce the multi-access interference, especially when the orthogonality of signature codes is degraded by the fading channel.

ADAPTIVE RECEIVERS FOR DIRECT-SPREAD AND MULTI-CARRIER CODE DIVISION MULTIPLE ACCESS SYSTEMS

by
Xiangqun Liu

A Thesis
Submitted to the Faculty of
New Jersey Institute of Technology
in Partial Fulfillment of the Requirements for the Degree of
Master of Science in Electrical Engineering

Department of Electrical and Computer Engineering

October 1994

APPROVAL PAGE

ADAPTIVE RECEIVER FOR DIRECT-SPREAD AND MULTI-CARRIER CODE DIVISION MULTIPLE ACCESS SYSTEM

Xiangqun Liu

Dr. Yeheskel Bar-Ness, Thesis Advisor — Date
Distinguished Professor of Electrical and Computer Engineering
New Jersey Institute of Technology

Dr. Nirwan Ansari, Committee Member — Date
Associate Professor of Electrical and Computer Engineering
New Jersey Institute of Technology

Dr. Zoran Siveski, Committee Member — Date
Assistant Professor of Electrical and Computer Engineering
New Jersey Institute of Technology

BIOGRAPHICAL SKETCH

Author: Xiangqun Liu

Degree: Master of Science in Electrical Engineering

Date: October 1994

Undergraduate and Graduate Education:

- Master of Science in Electrical Engineering,
  New Jersey Institute of Technology,
  Newark New Jersey, 1994
- Bachelor of Science in Electrical Engineering,
  Shanghai Jiao Tong University,
  Shanghai, P. R. China, 1988

Major: Electrical and Computer Engineering

This thesis is dedicated to my family.

ACKNOWLEDGMENT

I wish to express my sincere thanks to Dr. Yeheskel Bar-Ness, my advisor, for his guidance throughout my research.

Thanks also to Dr. Nirwan Ansari and Dr. Zoran Siveski for their advice and for serving as members of my committee.

Finally I would like to thank my family and friends for their support and encourgement during my stay at NJIT.

TABLE OF CONTENTS

Chapter Page

LIST OF FIGURES

Figure Page

CHAPTER 1

INTRODUCTION

In the mobile communication environment and the evolving personal communication networks, several techniques are used to transmit messages from different sources over a common medium. In addition to traditional multi-access techniques such as Time-Division Multiple Access (TDMA) and Frequency-Division Multiple Access (FDMA), Code-Division Multiple Access (CDMA) is an other technique which has been under intensive research recently.

In a communication system using CDMA, each user's signal is encoded with a pre-assigned signature code (signature sequence). Whenever the user has data to transmit, it can access the channel at any time and the encoded signals from different sources are transmitted through the same channel. Because of this multi-access method, the signal at one receiver of a particular user consists of three parts: the desired signal part which is intended to be received by the user, the residual interference part which is the multi-access interference from all other users and the white additive Gaussian noise (AWGN) from the channel. The purpose of the CDMA receiver is to separate the desired signal from the interference. We will discuss two kinds of CDMA, which differ by the spread spectrum technique used: Direct-Sequence (DS) spread spectrum CDMA and Multi-Carrier (MC) spread spectrum CDMA.

In the DS-CDMA system, each signal bit at the transmitter is multiplied by a high-speed time-variant signature sequence. Usually the resultant wideband sequence occupies the entire available bandwidth. The signature sequences are chosen to have good orthogonality. At the receiver end, the residual interference is proportional to the cross correlations between the signature sequences for the designated user and

those of other users, as well as the power of other users if signals do not suffer fading in the channel.

Many different methods have been proposed to separate the received DS-CDMA signals. The conventional receiver employs a bank of filters matched to the signature sequences of each user. The knowledge required for the conventional receiver is the power of the transmitted signals and the signature sequence of each user. Since the conventional method does not take into consideration the presence of multi-access interference, it is reliable only when there are few transmissions simultaneously. Furthermore, it is suitable only when the powers of the interference signals are relatively small. Otherwise the so called "near-far" problem will degrade the performance of the system.

An optimum receiver [1] has been designed to solve this problem. With the knowledge of the transmitted power of each user, a Viterbi algorithm is applied to separate the received signals optimally. The optimum receiver is proved to be "near-far" resistant, but its drawbacks are obvious. First, it requires the knowledge of the power of each user, which results in the increasing price of estimating the transmitted power. Second, the computational complexity increases exponentially with the number of users.

Some suboptimum receivers [2][3] are then proposed to reduce the computational complexity as well as to cope with the "near-far" problem. The two-stage decorrelating receiver is one of them [3]. The interference is estimated in the first stage, which is called the tentative decision stage. The tentative decisions are then weighed in the second stage and subtracted from the output of the matched filters. Therefore the performance is much better than that of the conventional receiver and the computational complexity is linear to the number of users. However, it still requires the knowledge of received signal powers and the weights are fixed to a function of these powers.

The idea of the adaptive DS-CDMA receiver [4] was inspired by the suboptimum two-stage decorrelating receiver. Instead of using fixed weights for the interference canceler, an adaptive algorithm is applied in the second stage. The weights are updated adaptively so as to converge to the optimal values, i.e., the weights are adjusted adaptively until the received signals are separated. In this receiver, the knowledge of transmitted powers are no longer required. The weights are determined by the observed results at the output of the receiver and the tentative decision stage. So, no prior knowledge of the *powers* of the transmitted signals is required. What it needs to know are only the *signature sequences*. This makes the receiver suitable for a power changing environment, which is a very important feature in mobile communications. The performance of the receiver depends on two things, the algorithm for controlling the weight updating in the second stage and the estimation of interference in the tentative decision stage.

When a *hard limiter* is applied in the tentative decision stage to estimate the interference, the error performance of the receiver is improved substantially in the presence of relatively strong interference. But when the power of the interference is relatively small, the performance is degraded by the use of the tentative decision stage. To solve this problem, *soft limiters* are introduced to the tentative decision stage [5][6]. These limiters preserve the same function as the hard limiter when the interference is relatively strong but modify the hard limiter function when interference is relatively small so that better estimations for interference can be achieved. In this thesis, we apply a new soft limiter—the *deadzone limiter*—to the adaptive DS-CDMA receiver. The setting of thresholds for these limiters is discussed and the error performance for the system using deadzone limiters is analyzed by comparing it with the scheme using hard limiters.

MC-CDMA is a new transmission method different from DS-CDMA. It incorporates both multi-carrier modulation, also called multi-tone modulation or

Orthogonal Frequency Division Multiplexing (OFDM) [7][8][9], and spread spectrum technique. Instead of multiplying the user signal by a time-variant sequence, it transmits the same user information bit on multiple subcarriers simultaneously. For each user the subcarriers are phase shifted with a 0 or π phase offset corresponding to the signature sequence of the user. The frequency spacing between different subcarriers is chosen properly to ensure the orthogonality among subcarrier signals. The signal transmitted by each subcarrier is narrowband in nature so no significant intersymbol interference occurs between successive bits.

An important reason for using MC-CDMA rather than DS-CDMA is to reduce the effect of channel dispersion. In an indoor radio communication environment, the multi-path dispersive channel is characterized as a time-dispersive, frequency selective fading channel. In a DS-CDMA system, in order to achieve optimal performance with channel fading, the reception of multiple resolvable paths must be considered. So a RAKE receiver is introduced to deal with this situation. A typical RAKE receiver contains multiple correlators, each synchronized to one particular resolvable path. However, no code exists to ensure that the partial correlation of any two resolvable paths is orthogonal. Optimum combining of all resolvable paths with (correlated) signal components from multiple users is a non-trivial problem in DS-CDMA. One common simplification is to assume that interference in different resolvable paths is independent, which allows the use of Maximum Ratio Combining of different paths in the RAKE receiver. Complexity rapidly grows if the receiver exploits the fact that multi-access or self-interference signals in successive taps of the RAKE receiver are correlated.

In MC-CDMA, channel dispersion results in a different attenuation of different subcarriers, but each of the subcarriers experiences only narrowband fading which is flat-flat; namely, no time and frequency dispersion. Thus, one may model the multipath channel in MC-CDMA as a random complex attenuation at each

subcarrier. In many cases, the envelope of attenuation is modeled to have Rayleigh distribution. The fading amplitudes of adjacent subcarriers are correlated [10], but become uncorrelated if the channel delay spread is large.

In an MC-CDMA receiver, coherent detectors are first used to detect signals at each subcarrier. The signal component of a particular user at each subcarrier is then extracted by utilizing the orthogonality of the signature codes between different users. These components can be weighed by a complex matrix to combine signal components at different subcarriers to ensue strong attenuation of interference given a reasonable signal-to-noise ratio. Several algorithms, such as maximum ratio combining [11] and Wiener filtering [12] can be used for this purpose. In this thesis, we will introduce an adaptive decorrelating receiver in which an adaptive decorrelating interference canceler is used for signal separation.

The organization of this thesis is as follows: Chapters 2 and 3 deal with the DS-CDMA receiver. For comparison, earlier works on multiple-user detection are briefly reviewed in Chapter 2 with emphasis on the CDMA adaptive receiver. In Chapter 3, the performance of systems using deadzone limiters are analyzed. An MC-CDMA receiver is discussed in Chapter 4. Simulations are performed for the analysis of error performance and results are presented. The fading channel models are also discussed.

CHAPTER 2

LITERATURE SURVEY AND PREVIOUS RESULTS FOR DS-CDMA RECEIVERS

2.1 Description of System Model

The DS-CDMA communication system discussed here is a synchronous downlink system; namely, multi transmission stations (users) transmit their information over a *common* channel to a single receiver station. This scenario in mobile communication corresponds to the situation that the end user receives transmission from the base station. The system consists of three parts: a transmitter, a channel and a receiver, as shown in Figure 2.1.

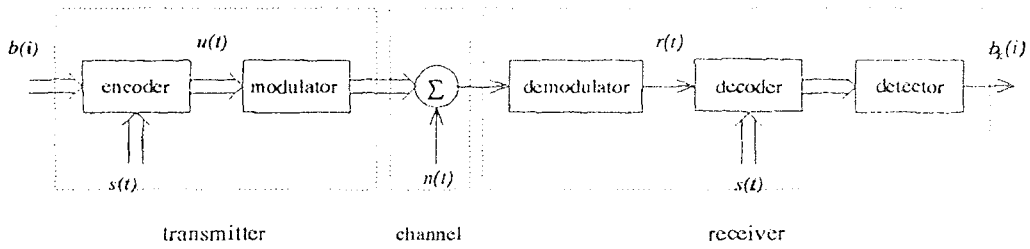

Figure 2.1 CDMA system model

2.1.1 Transmitter

At the transmitter of a K-user DS-CDMA system, the data bits for each station are transmitted by using a pre-assigned signature sequence to spread the spectrum of each data bit. For the k-th user ($1 \leq k \leq K$), the data signal is defined as

$$b_k(t) = \sum_{i=-\infty}^{\infty} b_k(i)\Pi_{T_b}(t - iT_b) \tag{2.1}$$

where $b_k(i) = \pm 1$ is the data symbol of the kth user at the ith time interval. Data sequences of different users are modeled to be independent and identically distributed

sequences ($i.i.d.$) with equally likely probabilities of $+1$ and -1; namely, $Pr\{b_k(i) = 1\} = Pr\{b_k(i) = -1\} = 1/2$. Π_T is a unit rectangular pulse defined as $\Pi_T = 1$ for $0 \leq t \leq T$, and $\Pi_T = 0$ otherwise. T_b is the symbol duration.

The signature sequence for the kth user is

$$s_k(t) = \sum_{j=-\infty}^{\infty} s_k(j)\Pi_{T_s}(t - jT_s) \tag{2.2}$$

where $s_k(j) = \frac{\pm 1}{\sqrt{T_b}}$ is the jth chip of the normalized signature sequence of the kth user. Each chip in the signature sequence has a duration of T_s and $T_s = T_b/N$. So each signature sequence contains N chips within one data symbol duration. As a result, the bandwidth needed to transmit the signal is $W = 1/T_s = N/T_b$. Each chip of the signature sequences is wideband and occupies the entire bandwidth of W. The cross and auto correlations for the signature sequences are defined as:

$$\begin{array}{l} \rho_{ij} = \int_0^{T_b} s_i(t)s_j(t)dt \quad \text{for } i, j = 1, 2, \cdots, K;\ i \neq j \\ \rho_{ii} = \int_0^{T_b} s_k^2(t)dt = 1 \end{array} \tag{2.3}$$

Obviously $\rho_{ij} = \rho_{ji}$.

In order to transmit the signal over the channel, the data signal of user k is first multiplied by its signature sequence to produce the baseband signal

$$u_k(t) = a_k b_k(t)s_k(t) \tag{2.4}$$

where a_k is the signal amplitude of the k-th user. Then the baseband signal is modulated to the carrier frequency:

$$v_k(t) = a_k u_k(t)cos(2\pi f_c t) \tag{2.5}$$

where f_c is the carrier frequency. In a synchronous DS-CDMA system, we assume there is no relative transmission time delay and no phase offset among different users. So, the transmitted signal at the input of the channel can be considered as the summation of all users' transmitted signals:

$$v(t) = \sum_{k=1}^{K} a_k b_k(t)s_k(t)cos(2\pi f_c t) \tag{2.6}$$

2.1.2 Channel

The channel for this DS-CDMA system is modeled as an additive white Gaussian noise (AWGN) channel with a double-side power spectral density of $\frac{N_0}{2}$. So, after the channel at the input of the receiver, we have $v(t) + N(t)$ as the received signal, where $N(t)$ is the channel's AWGN.

2.1.3 Receiver

The DS-CDMA receiver end consists of the demodulation, the matched filter bank followed by sampling and the interference canceler. After coherent demodulation, the received signal $r(t)$ is the summation of all the baseband signals plus noise.

$$\begin{aligned} r(t) &= \frac{2}{T_b}\int_0^{T_b} v(t)cos(2\pi f_c t)dt + \frac{2}{T_b}\int_0^{T_b} N(t)cos(2\pi f_c t)dt \\ &= \sum_{k=1}^{K} a_k b_k(t)s_k(t) + n(t) \\ &= \sum_{k=1}^{K}\sum_{i=-\infty}^{\infty} a_k b_k(i)\Pi_{T_b}(t - iT_b)s_k(t) + n(t) \end{aligned} \tag{2.7}$$

where $n(t)$ is the channel's AWGN. i stands for the ith time interval. Assuming the ideal case of no intersymbol interference, then the above equation can be simplified as

$$r(t) = \sum_{l=1}^{K} b_l(i)a_l s_l(t) + n(t) \tag{2.8}$$

If we let the k-th user be the designated user; namely, the user of current interest, we can write equation (2.8) by pulling out the data signal of the k-th user from the summation at time i:

$$r(t) = b_k(i)a_k s_k(t) + \sum_{\substack{l=1 \\ l\neq k}}^{K} b_l(i)a_l s_l(t) + n(t) \tag{2.9}$$

Obviously the received signal in the above equation consists of three parts:

1. The signal part of the k-th user,

2. The multiple access interferences from other users, and

3. The channel's AWGN.

The function of the receiver is to detect the k-th user, in another words, to separate the signal of the k-th user from the interference and the noise. We will divide DS-CDMA receiver in two categories: the non-adaptive receiver and adaptive receiver.

2.2 Non Adaptive CDMA Receivers

As introduced in Chapter 1, there are three kinds of non-adaptive receivers: conventional, optimum and suboptimum receivers. We will briefly review them in this section.

2.2.1 Conventional Receiver

A conventional receiver is also called a correlation receiver or a matched filter (MF) receiver. For the single-user case, the conventional receiver first processes the received signal with a matched filter. The matched filter is to match the signal waveform of the transmitted signal. As proven in communication theory, the matched filter can give us an optimal SNR performance in the presence of AWGN. So, in a K-user environment, the conventional receiver simply consists of K matched filters, with each matched to the signature sequence of a particular user. The K matched filters form a filter bank, as shown in Figure 2.2.

The output of the k-th matched filter and sampling is:

$$\begin{aligned} x_k(i) &= \int_0^{T_b} r(t)s_k(t)dt \\ &= a_k b_k(i) + \sum_{\substack{l=1 \\ l\neq k}}^{K} \rho_{lk} a_l b_l(i) + n_k(i) \end{aligned} \tag{2.10}$$

where

$$n_k(i) = \int_0^{T_b} n(t)s_k(t)dt \tag{2.11}$$

On the other hand, we can also use matrix presentations to show the receiving process. A column vector $\boldsymbol{b}(i) = [b_1(i), b_2(i), \cdots, b_K(i)]^T$ is used to represent the K

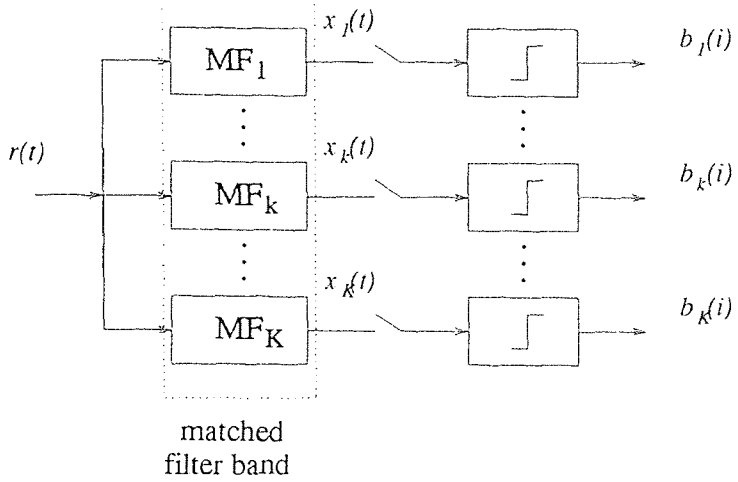

Figure 2.2 Conventional Receiver

users' data bits at the i-th time interval. A diagonal matrix $\boldsymbol{A} = \text{diag}[a_1, a_2, \cdots, a_K]$ represents the amplitudes of all the users. The cross correlation matrix of the signature sequences is

$$\boldsymbol{\mathcal{P}} = \begin{bmatrix} 1 & \rho_{12} & \cdots & \rho_{1K} \\ \rho_{21} & 1 & \cdots & \rho_{2K} \\ \vdots & \vdots & \ddots & \vdots \\ \rho_{K1} & \rho_{K2} & \cdots & 1 \end{bmatrix} \tag{2.12}$$

where ρ_{ij} is the cross correlation defined in equation (2.3). For the sake of convenience, the index i will be omitted elsewhere in this thesis when dealing with DS-CDMA. In this notation, the output vector of the matched filter bank is:

$$\boldsymbol{x} = \boldsymbol{\mathcal{P}} \boldsymbol{A} \boldsymbol{b} + \boldsymbol{n} \tag{2.13}$$

where $\boldsymbol{x} = [x_1, x_2, \cdots, x_K]^T$. The noise vector $\boldsymbol{n} = [n_1, n_2, \cdots, n_K]^T$ has a zero mean and a covariance matrix of $\boldsymbol{\Sigma}_n$.

$$\boldsymbol{\Sigma}_n = E\{\boldsymbol{n}\boldsymbol{n}^T\} = \frac{N}{2}\boldsymbol{\mathcal{P}} \tag{2.14}$$

The final decision for the k-th user is made by taking the sgn function of x_k, which still includes three parts: the signal part of the designated user, interference

from all other users, and noise.

$$\hat{b}_k = \mathrm{sgn}\{x_k\} = \mathrm{sgn}\{a_k b_k + \sum_{\substack{l=1 \\ l \neq k}}^{K} \rho_{lk} a_l b_l + n_k\} \tag{2.15}$$

Because the conventional receiver does nothing to cancel the superimposed interference, this kind of receiver is reliable only when the interference is small so as $\sum_{\substack{l=1 \\ l \neq k}}^{K} \rho_{lk} a_l b_l < a_k b_k$; namely, we should:

1. Limit the number of users,

2. Restrict the power of other users,

3. Use signature sequences with small cross correlations.

However, in practice, there are always some users close to the receiver which are much stronger than those which are far away. So, the user with small power is almost undetectable even if the cross correlations of the signature sequences are very small. This is the so called "near-far" problem, which is the major drawback of conventional receiver.

2.2.2 Optimum Receiver

The optimum receiver is to have a decision system after the conventional receiver to detect the transmitter signals (see Figure 2.3). There are two kinds of decision rules: the maximum likelihood (ML) method and the maximum a-posteriori probability (MAP) method [13].

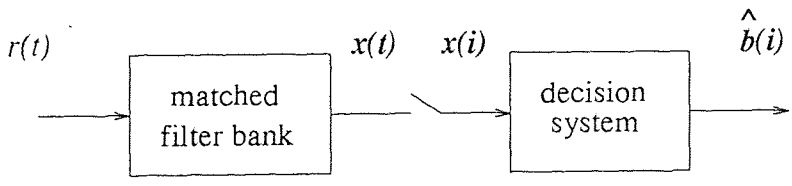

Figure 2.3 Block Diagram of Optimum Receiver

The optimum receiver can efficiently solve the "near-far" problem. However, its drawback is also obvious and impossible to be implemented in practice. It requires the prior knowledge of the signal powers. On the other hand, the computational complexity will increase exponentially with the number of users. But it can be used as a benchmark to measure the performance of different receiver schemes.

2.2.3 Suboptimum Receiver

Suboptimum receivers are proposed to achieve near-optimum performance with less computational complexity. For this purpose, it employs an interference canceler after the conventional receiver. There are several kinds of canceler that can be used. One of them is introduced in [3] for the two-stage decorrelating receiver. In the first stage, after the decorrelator which is represented by the function of $\mathcal{P}^{-1}$, sgn functions are used to make tentative decisions. These decisions are used as the estimations of transmitted data for all users. In the second stage, which is called interference canceler, the estimations for interference are weighed by a matrix W and subtracted from the outputs of the matched filter bank. The outputs of the second stage are the sgn of the subtraction results, which we call final decisions in comparison with the tentative decisions of the first stage. The two-stage non adaptive suboptimum DS-CDMA receiver is depicted in Figure 2.4

The output of the decorrelator is given as

$$\begin{aligned} \boldsymbol{z} &= \mathcal{P}^{-1}\boldsymbol{x} \\ &= \mathcal{P}^{-1}(\mathcal{P}\boldsymbol{A}\boldsymbol{b} + \boldsymbol{n}) \\ &= \boldsymbol{A}\boldsymbol{b} + \boldsymbol{\eta} \end{aligned} \tag{2.16}$$

where $\boldsymbol{z} = [z_1, z_2, \cdots, z_K]^T$. $\boldsymbol{x}$ is the output of the matched filter bank sampling described in equation (2.13). $\boldsymbol{\eta} = [\eta_1, \cdots, \eta_K]^T$ is K dimension Gaussian random

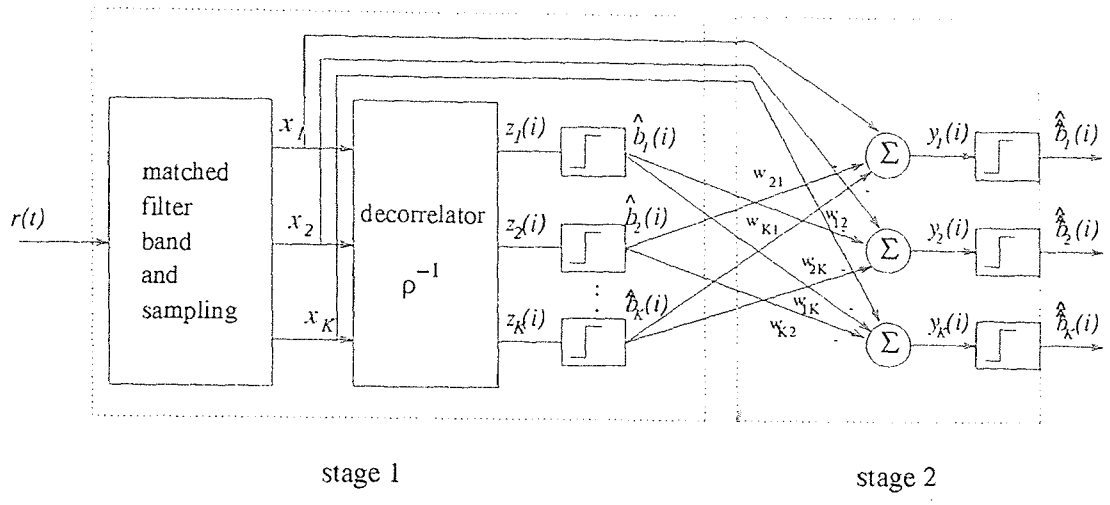

Figure 2.4 Suboptimum Receiver

vector with the mean vector and covariance matrix:

$$\begin{aligned} \boldsymbol{\mu}_\eta &= 0 \\ \boldsymbol{\Sigma}_\eta &= \tfrac{N}{2}\boldsymbol{\mathcal{P}}^{-1} \end{aligned} \tag{2.17}$$

So $\hat{\boldsymbol{b}} = sgn(\boldsymbol{z})$ will be a tentative interference-free estimation of the signal. Utilizing this estimation, the output of the interference canceler can be expressed as

$$\boldsymbol{y} = \boldsymbol{x} - \boldsymbol{W}^T\hat{\boldsymbol{b}} \tag{2.18}$$

where $\boldsymbol{W}$ is a $K \times K$ weight matrix with fixed weights of $\boldsymbol{W} = (\boldsymbol{\mathcal{P}} - \boldsymbol{I})\boldsymbol{A}$. The final decision is made from $\boldsymbol{y}$, the output of the second stage.

$$\hat{\hat{\boldsymbol{b}}} = \mathrm{sgn}(\boldsymbol{y}) \tag{2.19}$$

In a noise free environment, we will have $\hat{\boldsymbol{b}} = \boldsymbol{b}$. However, in a noisy environment, when the tentative decision of interferences are not correct; namely, $\hat{\boldsymbol{b}} = -\boldsymbol{b}$, then

$$\boldsymbol{y} = (2\boldsymbol{\mathcal{P}} - \boldsymbol{I})\boldsymbol{A}\boldsymbol{b} + \boldsymbol{\eta} \tag{2.20}$$

The interferences will be enhanced. The reason is because the weights are fixed. When the tentative decision is not correct, there is no feedback to make adjustment to

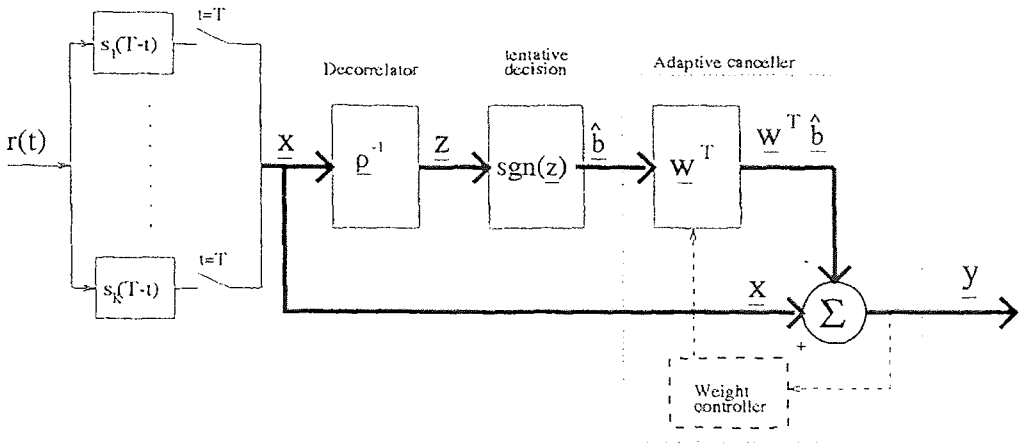

Figure 2.5 Adaptive Receiver

the weight matrix. On the other hand, the system still require the a prior knowledge of the signal power, as well as the signature sequence of each user.

2.3 Adaptive Receivers

Similar to a non-adaptive receiver, the adaptive CDMA receiver consists of a matched filter bank front end followed by sampling, a decorrelator and a tentative decision stage. The difference is that the interference canceler is adaptive in the adaptive receiver. The layout of the adaptive receiver is shown in Figure 2.5. Compared with the two-stage non adaptive receiver in Figure 2.4, the adaptive receiver uses a mechanism to update the weights adaptively, while for non adaptive receiver the weights are fixed. The estimation of interference from the tentative decision stage are still weighed and subtracted from the desired signal. The weights are updated every time interval according to the feedback of the canceler's outputs of the previous time bit. So, the receiver can have optimal performance even when the signal power is changed with time. As a result, it does not need the a priori knowledge of signal power which is the major drawback of the non-adaptive receiver. This kind of signal separation is usually categorized as "blind separation".

Several criteria can be used for the adaption of the weights. Minimum power is one of them [4][14]. It employs a steepest descent algorithm and minimizes the power of the outputs of the adaptive canceler simultaneously.

Define the weight matrix of the adaptive canceler as:

$$\boldsymbol{W} = \begin{bmatrix} 0 & w_{12} & \cdots & w_{1K} \\ w_{21} & 0 & \cdots & w_{2K} \\ \vdots & \vdots & \ddots & \vdots \\ w_{K1} & w_{K2} & \cdots & 0 \end{bmatrix} \tag{2.21}$$

where w_{ji} indicates the weight of the interference from user j to user i. The output of the adaptive canceler for the k-th user can be expressed as

$$y_k = x_k - \boldsymbol{w}_k^T \hat{\boldsymbol{b}}_k \tag{2.22}$$

where $\boldsymbol{w}_k$ is the k-th column vector of the weight matrix $\boldsymbol{W}$ with the k-th element w_{kk} deleted, and $\hat{\boldsymbol{b}}_k$ is the vector obtained from the tentative decisions $\hat{\boldsymbol{b}}$ by deleting the element $\hat{b}_k$. By using minimum power criteria, the optimum weight w_{jk} can be obtained by iterative search:

$$w_{lk} \leftarrow w_{lk} - \frac{\mu \partial}{\partial w_{lk}} E\{y_k^2\} \tag{2.23}$$

which is the same as

$$w_{lk} \leftarrow w_{lk} + \mu E\{y_k \hat{b}_l\} \tag{2.24}$$

where μ is the learning step of the adaptive canceler. From equations (2.22) and (2.24) we can see that w_{lk} is adapted every time interval. The adaption is guided by the cross correlation of the canceler's output y_k and the interference estimation $\hat{b}_l$. The optimum value of w_{lk} is achieved when $E\{y_k \hat{b}_l\} = 0$; namely, the canceler output of the designated user y_k is totally decorrelated with the interference estimation $\hat{b}_l$. The convergence of the system using minimum power criteria has been proved [14].

CHAPTER 3

RECEIVER USING TENTATIVE DECISION

The performance of the receiver depends on many factors. In this chapter, we will focus on the effect of tentative decisions on the error performance. As discussed in section 2.2.3, the final decisions are affected by the tentative decisions in the two-stage non adaptive receiver. For the adaptive receiver case, the adaption of weights is also affected by the tentative decisions. The functions used in the tentative decision stage for estimating the interference are called limiters. Two kinds of tentative decision schemes are discussed in this chapter, hard limiters and deadzone limiters. We will also compare the performance of these two schemes.

3.1 Receiver Using Hard Limiters

In the adaptive receiver discussed in section 2.3, *sign* functions are used to make the tentative decisions. They are the so called hard limiters. The output vector of the tentative decision stage is:

$$\hat{\boldsymbol{b}} = sgn(\boldsymbol{z}) \tag{3.1}$$

with $\boldsymbol{z}$ given in equation (2.16). Thus the estimation of interference depends only on the polarities of the decorrelated signals. The presence of noise $\boldsymbol{\eta}$ could make the estimation incorrect. If the SNRs are large enough, most of the time the correct estimation could be obtained from the tentative decision stage. However, if the relative signal powers are not strong enough, the estimation will be dominated by the AWGN.

Figure 3.1 shows the error performance of a two-user receiver using hard limiters in comparison with that of the adaptive receiver without a tentative decision stage. The SNR of the designated user is $SNR_1 = 10dB$. The relative SNR of interference

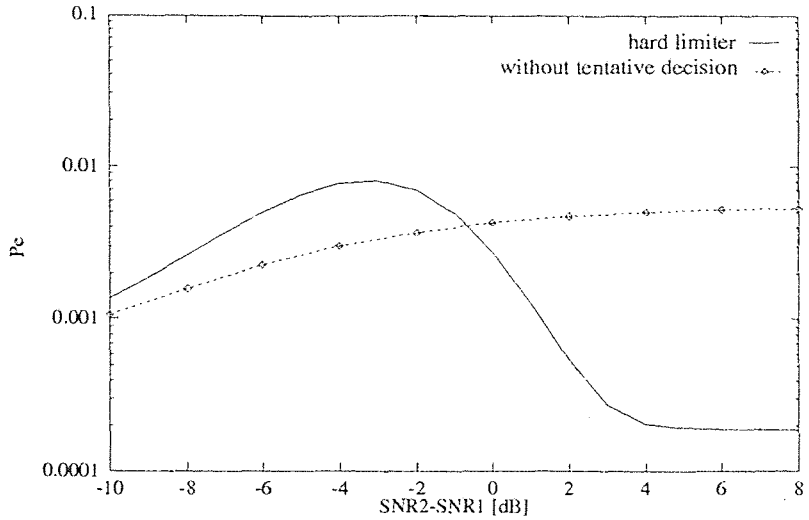

Figure 3.1 The Performance of the Hard Limiter Receiver

$(SNR_2 - SNR_1)$ is varied, as indicated by the horizontal axis. The vertical axis shows the probability of error of user 1. From this Figure we can see that the performance of the hard limiter receiver is much better than the linear adaptive receiver especially when interference is relatively strong. The result certainly makes sense because when the signal power of interference is relatively higher than that of the designated user, the polarities of the decorrelated signals are dominated by the interference so that the tentative decision can give the correct estimation of the interference and thus lead to a correct attempt at weights updating.

However, when the power of interference is relatively small, using a hard limiter will degrade the error performance. The reason is that when the interference is relatively small, the estimation of interference will be dominated by noise, which will give a wrong estimation of the interference. Thus the wrong estimation can lead the weight updating to a wrong direction. Consequently, more errors are introduced than without any interference cancellation. If other functions can be used when the interference is relatively small so that interference can be better estimated, we will be sure to have some improvement in error performance.

3.2 Receiver Using Deadzone Limiters

3.2.1 Receiver Model

The discussion in the previous section leads to the use of other limiters, especially when interference is small. To improve the receiver's performance, some modification should be introduced to the receiver scheme. One approach is to replace hard limiters with other kinds of limiters. When the power of interference is relatively high, these limiters will have the same function as a hard limiter; when the interference power is small, they will use some other functions to estimate the interference. The *soft limiter* is introduced for this purpose. Two kinds of non-hard limiters are presented in Figure 3.2. These limiters have similar properties: they modify the hard limiter function when the input is inside a small region ($|z_l| < t_{lk}$) and preserve the hard limiter property when the input is outside this region. A receiver using soft limiters was discussed in [6]. In this thesis, We will focus on the deadzone limiter shown in Figure 3.2(a).

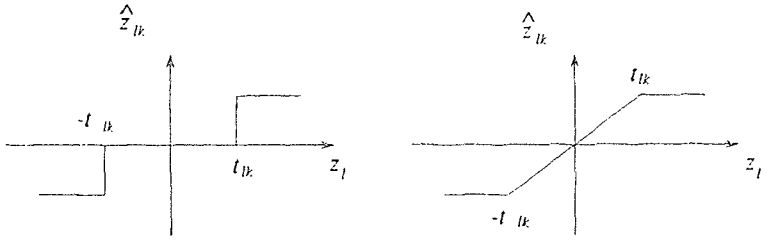

Figure 3.2 Soft limiters

A deadzone limiter has a small region called the *deadzone*. When the input is inside its deadzone, the output is zero. Outside this deadzone, it has the same function as a hard limiter. When the deadzone limiters are used instead of the hard limiters, the decision making procedure in the tentative decision stage will work this way: when the interference is strong , i.e., the input to the tentative decision stage is outside the deadzone, the tentative decision stage estimates the interference

according to the polarities of its input; when the interference is small, the input is inside the deadzone, and the branch of the adaptive canceler is disabled. This satisfies the argument in section 3.1. The receiving scheme using deadzone limiters is shown in Figure 3.3. The function of the deadzone limiter in Figure 3.2(a) is

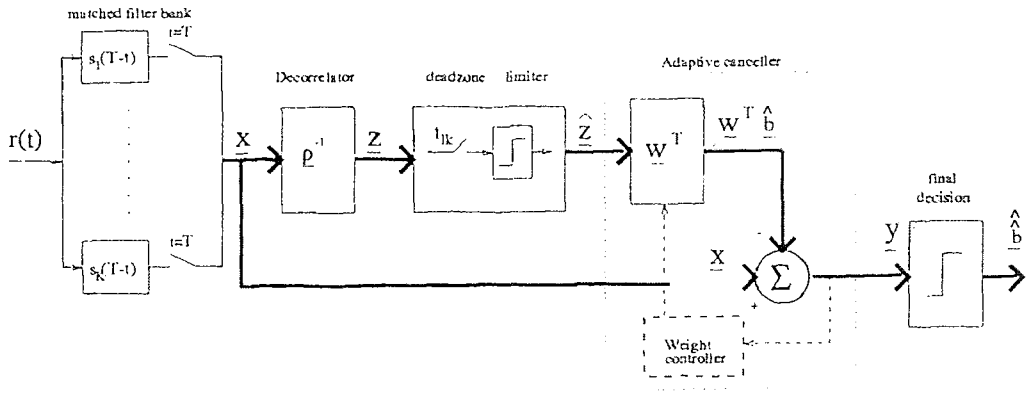

Figure 3.3 Deadzone Limiter Receiver

$$\hat{z}_{lk} = \begin{cases} 0; & |z_l| < t_{lk} \\ sgn(z_l) = \hat{b}_l; & \text{otherwise} \end{cases} \tag{3.2}$$

with the variables interpreted as

z_l : the l-th element of $\boldsymbol{z}$ described in equation (2.16); namely, the signal of user l after the decorrelator.

$\hat{z}_{lk}$: the output of the deadzone limiter estimating the interference from user l to user k.

t_{lk} : the threshold used in the above deadzone limiter to set its deadzone.

Since the signal from user l will produce interference for all other users, we need K deadzone limiters for z_l in a tentative decision stage to estimate the interference. So we will have $K \times K = K^2$ limiters in total. Obviously $\hat{z}_{kk} \equiv 0$. In matrix notation,

the output of the tentative decision stage is

$$\hat{\boldsymbol{Z}} = \begin{bmatrix} 0 & \hat{z}_{12} & \cdots & \hat{z}_{1K} \\ \hat{z}_{21} & 0 & \cdots & \hat{z}_{2K} \\ \vdots & \vdots & \ddots & \vdots \\ \hat{z}_{K1} & \hat{z}_{K2} & \cdots & 0 \end{bmatrix} \tag{3.3}$$

with $\hat{z}_{ij}$ given in equation 3.2 for $i, j = 1, 2, \cdots, K$.

Based on the interference estimation, the output of the interference canceler for designated user k is :

$$\begin{aligned} y_k &= x_k - \boldsymbol{w}_k^T \hat{\boldsymbol{z}}_k \\ &= x_k - \sum_{\substack{l=1 \\ l \neq k}}^{K} w_{lk} \hat{z}_{lk} \end{aligned} \tag{3.4}$$

where $\hat{\boldsymbol{z}}_k$ is the k-th column of $\hat{\boldsymbol{Z}}$ with $\hat{z}_{kk}$ deleted. The optimum weights can be obtained by the iterative search:

$$\boldsymbol{w}_k(i+1) = \boldsymbol{w}_k(i) - \frac{\mu}{2} \frac{\partial}{\partial \boldsymbol{w}_k(i)} E\{y_k^2(i)\} \tag{3.5}$$

3.2.2 Optimal Weights

The optimum weights in steady state can be obtained by setting the second item of equation 3.5 to zero, that is, minimizing the power of the output simultaneously.

$$\frac{\partial}{\partial \boldsymbol{w}_k} E\{y_k^2\} = 0 \tag{3.6}$$

From equation (3.4) we have:

$$\begin{aligned} \frac{\partial}{\partial \boldsymbol{w}_k} E\{y_k^2\} &= E\{2y_k \frac{\partial y_k}{\partial \boldsymbol{w}_k}\} \\ &= E\{-2y_k \hat{\boldsymbol{z}}_k\} \\ &= -2E\{x_k \hat{\boldsymbol{z}}_k\} + 2E\{\hat{\boldsymbol{z}}_k \hat{\boldsymbol{z}}_k^T\} \boldsymbol{w}_k \end{aligned} \tag{3.7}$$

Using equation (3.6) and (3.7), we have:

$$E\{y_k \hat{\boldsymbol{z}}_k\} = E\{x_k \hat{\boldsymbol{z}}_k\} - E\{\hat{\boldsymbol{z}}_k \hat{\boldsymbol{z}}_k^T\} \boldsymbol{w}_k = 0 \tag{3.8}$$

So, the optimum weight vector can be evaluated as:

$$\boldsymbol{w}_k = \left[E\{\hat{\boldsymbol{z}}_k \hat{\boldsymbol{z}}_k^T\}\right]^{-1} E\{x_k \hat{\boldsymbol{z}}_k\} \tag{3.9}$$

According to equation (2.13), we have

$$\begin{aligned} x_k &= a_k b_k + \sum_{\substack{l=1 \\ l \neq k}}^{K} \rho_{lk} a_l b_l + n_k \\ &= a_k b_k + \boldsymbol{\rho}_k^T A_k \boldsymbol{b}_k + n_k \end{aligned} \tag{3.10}$$

where $\boldsymbol{A}_k$ is obtained from $\boldsymbol{A}$ with the k-th row and column deleted, $\boldsymbol{\rho}_k$ is the k-th column vector of $\mathcal{P}$ with the k-th element deleted. Also from equation (3.2), we know that $\hat{\boldsymbol{z}}_k$ is a function of $(\boldsymbol{A}_k \boldsymbol{b}_k + \boldsymbol{n}_k)$. Because the information data bits are i.i.d., and the noise is uncorrelated with the data bits, we have

$$\begin{aligned} E\{x_k \hat{\boldsymbol{z}}_k\} &= E\{(a_k b_k + \boldsymbol{\rho}_k^T \boldsymbol{A}_k \boldsymbol{b}_k + n_k)\hat{\boldsymbol{z}}_k \\ &= E\{\hat{\boldsymbol{z}}_k \boldsymbol{b}_k^T\} \boldsymbol{A}_k \boldsymbol{\rho}_k \end{aligned} \tag{3.11}$$

Together with equation (3.9), we have

$$\boldsymbol{w}_k = \left[E\{\hat{\boldsymbol{z}}_k \hat{\boldsymbol{z}}_k^T\}\right]^{-1} E\{\hat{\boldsymbol{z}}_k \boldsymbol{b}_k^T\} \boldsymbol{A}_k \boldsymbol{\rho}_k \tag{3.12}$$

The detail derivation of the expectation values of the above equation for two and three user cases are given in Appendix A.

3.2.3 Setting of Thresholds

The setting for the "best" thresholds is obtained heuristically from experiments. Several threshold settings are used in the experiments:

$$t_{ik}^{(1)} = \frac{\rho_{ik}^2 E^2\{|z_k|\}}{E\{|z_i|\}}$$

$$t_{ik}^{(2)} = \frac{\rho_{ik} E\{|z_k|\}}{E\{|z_i|\}}$$

$$t_{ik}^{(3)} = \frac{\rho_{ik} E^2\{|z_k|\}}{E\{|z_i|\}}$$

$$t_{ik}^{(4)} = \frac{\rho_{ik} E^2\{|z_k|\}}{E^2\{|z_i|\}}$$

$$t_{ik}^{(5)} = \frac{\rho_{ik} E\{|z_k|\}}{E^2\{|z_i|\}}$$

The expectation $E\{|z_k|\}$ in the above equations is evaluated as:

$$\begin{aligned} E\{|z_k|\} &= E\{|a_k b_k + \eta_k|\} \\ &= a_k \left(1 - 2Q\left(\frac{a_k}{\sigma_{\eta_k}}\right)\right) + \frac{2\sigma_{\eta_k}}{\sqrt{2\pi}} e^{-\frac{a_k^2}{2\sigma_{\eta_k}^2}} \end{aligned} \tag{3.13}$$

where a_k is the amplitude of the k-th user's transmitted signal, σ_{η_k} is the variance of Gaussian noise η_k defined in equation (2.17) and $Q(x)$ is the error function:

$$Q(x) = \frac{1}{2\pi} \int_x^\infty e^{\frac{x^2}{2}} dx \tag{3.14}$$

The analytical error probabilities using these settings will be discussed in section 3.3.

3.2.4 Error Probabilities

The final decision for the designated user k is made at the output of the interference canceler:

$$\hat{\hat{b}}_k = sgn(y_k) \tag{3.15}$$

With y_k given in equation (3.4), together with equation (2.10), we have

$$\begin{aligned} \hat{\hat{b}}_k &= \text{sgn}(x_k - \boldsymbol{w}_k^T \hat{\boldsymbol{z}}_k) \\ &= \text{sgn}(a_k b_k + \boldsymbol{\rho}_k \boldsymbol{A}_k \boldsymbol{b}_k + n_k - \boldsymbol{w}_k^T \hat{\boldsymbol{z}}_k) \end{aligned} \tag{3.16}$$

Error occurs when the final decision of the receiver is different from the transmitted information bit; namely, $\hat{\hat{b}}_k \neq b_k$. The probability of this error occurrence is conditioned on three things: the information bits of the designated user b_k, the information bits of the interference $\boldsymbol{b}_k$ and the estimation of the interference $\hat{\boldsymbol{z}}_k$, that is

$Pr\{\hat{\hat{b}}_k \neq b_k | b_k, \boldsymbol{b}_k, \hat{\boldsymbol{z}}_k\}$. The probability of error is the expected value of this probability over this condition region.

$$Pe_k = E_{b_k, \boldsymbol{b}_k, \hat{\boldsymbol{z}}_k} Pr\{\hat{\hat{b}}_k \neq b_k | b_k, \boldsymbol{b}_k, \hat{\boldsymbol{z}}_k\} \tag{3.17}$$

Because the bits of interference $\boldsymbol{b}_k$ are binary distributed i.i.d. random variables, there are totally 2^{K-1} combinations of $\boldsymbol{b}_k$ with equal probability of $\frac{1}{2^{K-1}}$. The above equation becomes

$$Pe_k = \frac{1}{2^{K-1}} \sum_{\boldsymbol{b}_k} E_{\hat{\boldsymbol{z}}_k} Pr\{(\hat{\hat{b}}_k \neq b_k) | b_k, \hat{\boldsymbol{z}}_k\} \tag{3.18}$$

Similarly, consider the binary distribution of the b_k, we have

$$\begin{aligned} Pr\{\hat{\hat{b}}_k \neq b_k | b_k\} &= \frac{1}{2} Pr\{b_k = 1, \hat{\hat{b}}_k = -1\} + \frac{1}{2} Pr\{b_k = -1, \hat{\hat{b}}_k = 1\} \\ &= Pr\{b_k = -1, \hat{\hat{b}}_k = 1\} \end{aligned} \tag{3.19}$$

Hence the error probability of user k can be written as:

$$Pe_k = \frac{1}{2^{K-1}} \sum_{\boldsymbol{b}_k} E_{\hat{\boldsymbol{z}}_k} Pr\{b_k = -1, \hat{\hat{b}}_k = 1 | \hat{\boldsymbol{z}}_k\} \tag{3.20}$$

Combining equation (3.20) on (3.16):

$$Pe_k = \frac{1}{2^{K-1}} \sum_{\boldsymbol{b}_k} E_{\hat{\boldsymbol{z}}_k} Pr\{n_k > a_k - \boldsymbol{b}_k^T \boldsymbol{A}_k \boldsymbol{\rho}_k + \boldsymbol{w}_k^T \hat{\boldsymbol{z}}_k | \hat{\boldsymbol{z}}_k\} \tag{3.21}$$

The $(K-1) \times 1$ vector $\boldsymbol{z}_k$ forms a $K-1$ dimensional hyper space for each particular combination of $\boldsymbol{b}_k$. In each dimension z_i $(i = 1, 2, \cdots, K, i \neq k)$, a deadzone limiter with a threshold is t_{ik} is used to estimate the interference from the i-th interference to the designated user k. Each axis of the hyper space is divided into three regions by its threshold. So, the $K-1$ thresholds divide the hyper space into M sub-regions $(M = 3^{K-1})$. Each sub-region D_m $(m = 1, 2, \cdots, M)$ has its corresponding $\hat{\boldsymbol{z}}_k$ combination $(\hat{\boldsymbol{z}}_k)_m$. Equation (3.21) is calculated by combining each individual sub-region.

$$Pe_k = \frac{1}{2^{K-1}} \sum_{\boldsymbol{b}_k} \sum_{m=1}^{M} Pr\{n_k > a_k - \boldsymbol{b}_k^T \boldsymbol{A}_k \boldsymbol{\rho}_k + \boldsymbol{w}_k^T (\hat{\boldsymbol{z}}_k)_m, \boldsymbol{z}_k \in D_m\} \tag{3.22}$$

Noticing that n_k is uncorrelated with $\boldsymbol{z}_k$, we have:

$$Pe_k = \frac{1}{2^{K-1}} \sum_{\boldsymbol{b}_k} \sum_{m=1}^{M} Pr\{n_k > a_k - \boldsymbol{b}_k^T \boldsymbol{A}_k \boldsymbol{\rho}_k + \boldsymbol{w}_k^T (\hat{\boldsymbol{z}}_k)_m\} Pr\{\boldsymbol{z}_k \in D_m\} \tag{3.23}$$

The first probability in the above equation can be evaluated by:

$$Q_m = Q\left(\frac{a_k - \boldsymbol{b}_k^T \boldsymbol{A}_k \boldsymbol{\rho}_k + \boldsymbol{w}_k^T (\hat{\boldsymbol{z}}_k)_m}{\sigma_{n_k}}\right) \tag{3.24}$$

where $Q()$ is the error function as defined in equation (3.14). In calculating the second probability, we introduce a Gaussian random vector $\boldsymbol{\eta}_k$ which can be obtained from $\boldsymbol{\eta}$ defined in equation (2.17) with the k-th element η_k deleted. The $(K-1)$ joint Gaussian density function for $\boldsymbol{\eta}_k$ is defined as $\boldsymbol{f}_{\boldsymbol{\eta}_k}$. Then, the second probability can be written as:

$$Pr\{\boldsymbol{z}_k \in D_m\} = \int_{D_m} \boldsymbol{f}_{\boldsymbol{\eta}_k} d\boldsymbol{\eta}_k \tag{3.25}$$

The integral has to be done in all sub-region D_m. For the m-th sub-region, we have $\boldsymbol{z}_k \in D_m$; namely,

$$\begin{cases} -t_{ik} - a_i b_i < \eta_i < t_{ik} - a_i b_i, & |z_i| < t_{ik} \\ \eta_i \geq t_{ik} - a_i b_i, \ \eta_i \leq -t_{ik} - a_i b_i; & \text{otherwise,} \end{cases} \tag{3.26}$$

for $i = 1, 2, \cdots, K$, $i \neq k$. Hence the error probability of the k-th user is:

$$Pe_k = \frac{1}{2^{K-1}} \sum_{\boldsymbol{b}_k} \sum_{m=1}^{M} Q_m \int_{D_m} \boldsymbol{f}_{\boldsymbol{\eta}_k} d\boldsymbol{\eta}_k \tag{3.27}$$

It should be brought to attention that there exists a 2^{K-1} hyper space base on different $\boldsymbol{b}_k$ combinations. Each hyper space has 3^{K-1} sub-regions separated by the deadzone thresholds. So, Pe_k should be evaluated over 6^{K-1} of sub-regions. The detailed calculations of error probabilities for 2-and-3 user cases are given in Appendix B. The computational complexity will increase exponentially with the number of users.

3.3 Performance Analysis

Using the five settings of threshold discussed in section 3.2.3, the analytic error performance for the two-users case, with cross correlation $\rho_{12} = 0.5$, is shown in Figure 3.4.

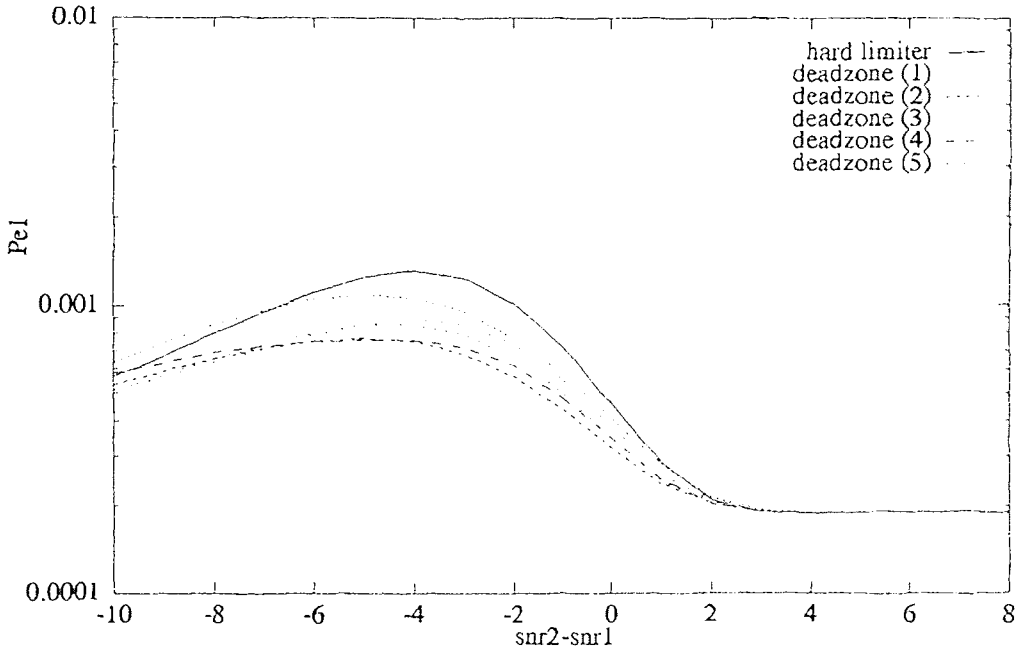

Figure 3.4 Error performance of user 1 (2 users, $\rho_{12} = 0.5$, $SNR_1 = 10dB$)

We can see from the figure that with a proper setting of the threshold, the error performance will be improved, especially for the peak value when $SNR_2 - SNR_1$ is around $-3dB$. When the interference becomes strong, the system performance will finally approach that of the single user in a white noise environment. Obviously the best performance is achieved when the threshold is set to $t^{(2)}$. Another experiment with a larger cross correlation of $\rho_{12} = 0.7$ also leads to the same conclusion (see Figure 3.5).

Similarly in the three-user case, Figure 3.6 shows the error performances of user 1 with the five settings of threshold. We use 7-chip Gold codes as the signature

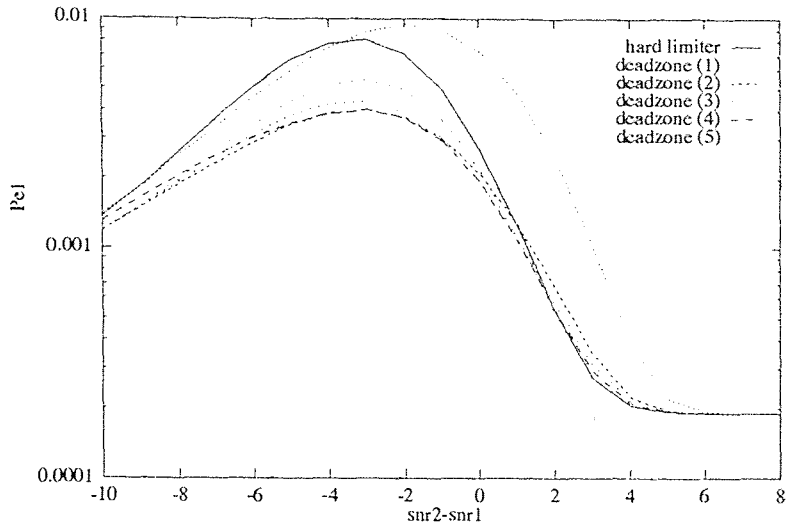

Figure 3.5 Error performance of user 1 (2 users, $\rho_{12} = 0.7$, $SNR_1 = 10dB$)

sequences. The cross correlation matrix is

$$\mathcal{P} = \frac{1}{7}\begin{bmatrix} 7 & -1 & 3 \\ -1 & 7 & -1 \\ 3 & -1 & 7 \end{bmatrix}$$

The simulation results for 2-and-3 user cases, with the setting $t^{(2)}$, are shown in Figure 3.7 and 3.8. Performances for the receiver using hard limiters are also plotted as a comparison.

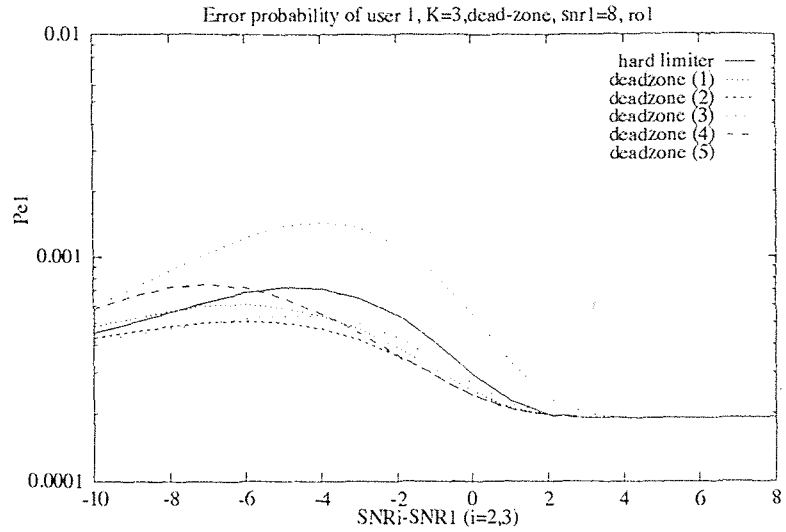

Figure 3.6 Error performance of user 1 (3 users, Gold codes, $SNR_1 = 10dB$)

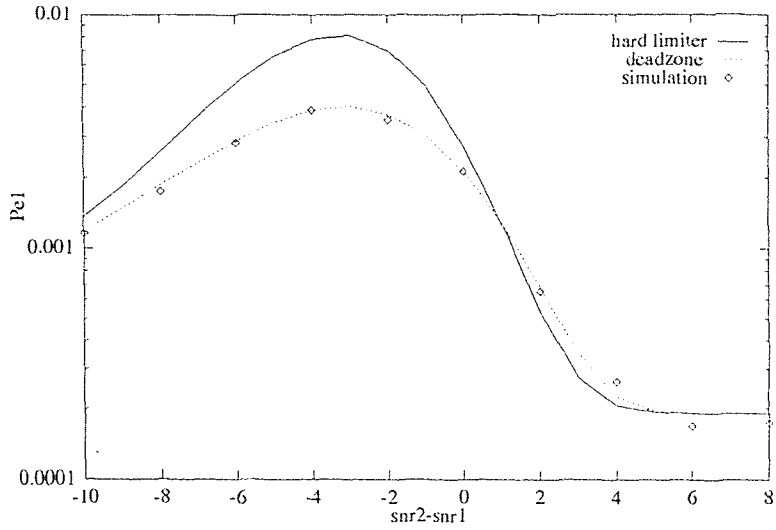

Figure 3.7 Error performance of user 1 (2 users, $\rho = 0.7$, $SNR_1 = 10dB$)

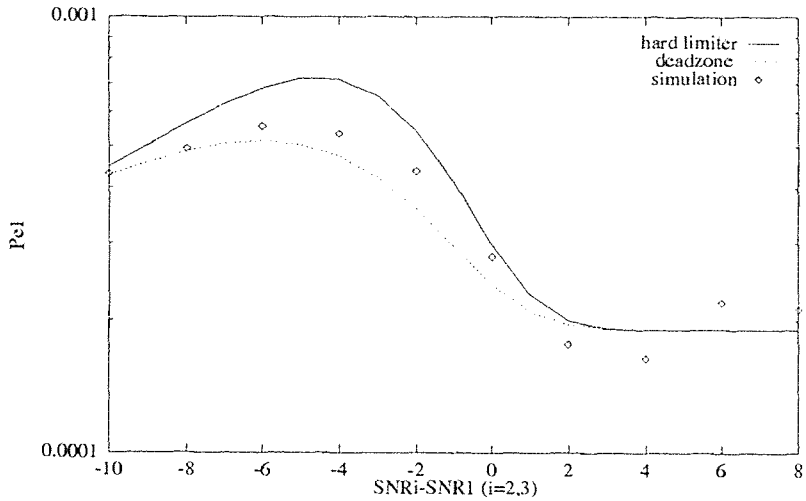

Figure 3.8 Error performance of user 1 (3 users, Gold codes, $SNR_1 = 10dB$)

CHAPTER 4

SYNCHRONOUS MC-CDMA SYSTEM WITH FADING CHANNEL AND DECORRELATING RECEIVER[1]

As discussed in the preceding chapters, DS-CDMA signals are encoded by multiplying each user's data symbol with its signature sequence in the time domain. The DS-CDMA signal is wideband and occupies the whole transmission bandwidth M/T_b, where T_b is the symbol duration and M is the number of chips in the signature sequences.

MC-CDMA uses a new transmission method different from DS-CDMA. With MC-CDMA, each data bit is transmitted simultaneously over multiple narrowband subcarriers. The user's signal at each subcarrier has a time-constant phase offset of 0 or π depending on its signature sequences. Hence, compared with DS-CDMA, MC-CDMA signals are encoded in the frequency domain. At each subcarrier, the MC-CDMA signal is narrowband with a bandwidth of $1/T_b$.

This difference leads to two important reasons for using MC-CDMA rather than DS-CDMA. First, the signal at each subcarrier is narrowband in nature, so no significant intersymbol interference occurs between successive bits. Second, it is easy to reduce the effect of channel dispersion as only narrowband fading occurs at each subcarrier.

A downlink MC-CDMA system with a Rayleigh fading channel and a decorrelating interference canceler will be discussed in the following sections.

---

[1] System modeling and analysis was performed in special communication by Dr. Yeheskel Bar-Ness.

4.1 Description of System Model

An MC-CDMA system consists of the same three parts as discussed in the DS-CDMA system: a transmitter, a channel, and a receiver. In addition to the common spread spectrum CDMA technique, the transmitting and receiving processes of MC-CDMA use multi-carrier modulation, also called multi-tone modulation or Orthogonal Frequency Division Multiplexing (OFDM). The channel is modeled as a time dispersive, frequency selective fading channel, which is the typical case for indoor radio communications.

4.1.1 Transmitter

Consider an MC-CDMA transmitter with K users and signature sequences of length M. The generation of the k-th user's transmitted signal can be described as follows. As shown in Figure 4.1, a single data bit of user k is first replicated into M parallel copies. Each copy is multiplied by one chip of the k-th user's signature sequence and then binary phase-shift keying (BPSK) modulated to a subcarrier to form a subcarrier signal. The m-th subcarrier signal for the k-th user is:

$$s_{k,m}(t) = b_k(i)\Pi_{T_b}(t - iT_b)c_k(m)\cos 2\pi(f_c + \frac{m-1}{T_b}F)t \tag{4.1}$$

where $b_k(i) = \pm 1$ is the i-th data bit of the k-th user and $\Pi_{T_b}(t)$ is the unit rectangular pulse. T_b is the symbol duration. They are the same as defined in section 2.1.1 for the DS-CDMA transmitter. $c_k(m) = \pm\frac{1}{\sqrt{M}}$, for $m = 1, 2, \cdots, M$ is the normalized signature sequence of the k-th user.

The frequency space between neighboring subcarriers is an integer multiple of the inverse of the data symbol time, F/T_b, where F is an integer number. f_c is the carrier frequency and we have $f_c \gg MF/T_b$. For different subcarrier signals, we have

$$\begin{aligned}\int_0^{T_b} s_{k,m}s_{k,l}dt &= \int_0^{T_b} b_k(i)^2 c_k(m)c_k(l)cos2\pi(f_c + \frac{m-1}{T_b}F)t\ cos2\pi(f_c + \frac{l-1}{T_b}F)tdt \\ &= 0 \end{aligned} \tag{4.2}$$

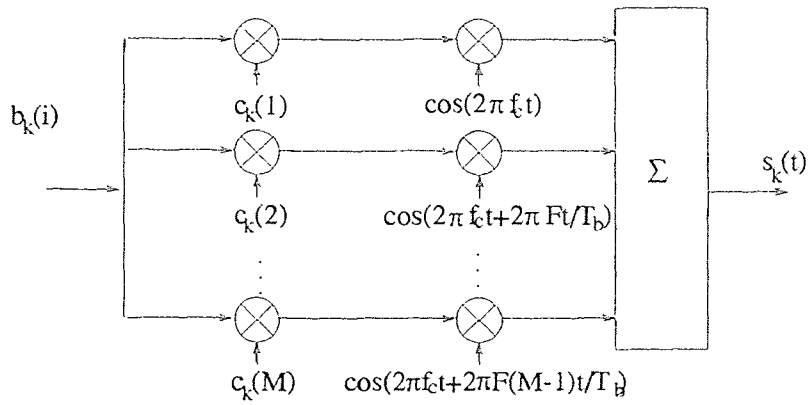

Figure 4.1 MC-CDMA transmitter model

Obviously the subcarrier signals are orthogonal to each other for any integer F. The transmitted signal of the k-th user at the i-th bit is the summation of all the corresponding subcarrier signals.

$$s_k(t) = b_k(i)\Pi_{T_b}(t - iT_b) \sum_{m=1}^{M} c_k(m) \cos 2\pi (f_c + \frac{m-1}{T_b} F)t \tag{4.3}$$

The total transmission bandwidth of the MC-CDMA signal $s_k(t)$ is MF/T_b. This bandwidth is minimized when $F = 1$, which applies OFDM on a Direct-Sequence spread-spectrum signal [15]. This is the case discussed in this thesis. However, larger values of F may be desired to further increase the transmission bandwidth, i.e., to achieve a larger frequency diversity gain without increasing the complexity in signal procession.

In matrix notation, the signature sequences for all the users form a code matrix

$$\boldsymbol{C} = [\boldsymbol{c}_1, \boldsymbol{c}_2, \cdots, \boldsymbol{c}_K] \tag{4.4}$$

where the column vector $\boldsymbol{c}_k = [c_k(1), c_k(2), \cdots, c_k(M)]^T$ represents the code for user k.

4.1.2 Fading Channel Model

The channel model used for the DS-CDMA system in the previous chapters is an AWGN channel while the effect of channel dispersion is not considered. However this AWGN channel is too idealistic to be used in a practical mobile communication environment. In practice, channel fading is always an unavoidable factor which can seriously degrade the performance of the communication system. Fading channel models will be introduced in this section.

4.1.2.1 Classification of Channels

The channel fading comes from the fact that there exists certain spreads in the physical medium of the channel. There are two kinds of spread to be considered in a dispersive medium, the Doppler spread and multipath spread. Doppler spread B_D is the spread in frequency, while multipath spread T_M is in time. In a strict sense a channel is dispersive both in time and in frequency. However, we can classify a channel's characteristics based upon the signal duration T and transmission bandwidth W[16].

I. Non-dispersive Channels:

A fading channel is considered non-dispersive if the two spreads meet the following conditions:

$$B_D \ll \frac{1}{T} \quad \text{and} \qquad T_M \ll \frac{1}{W}$$

A non-dispersive fading channel is also called a *flat-flat fading channel.* Define the channel fading as a function of time and frequency, $H(f,t)$, and we have:

$$H(f_1,t) = H(f_2,t) = h(t) \tag{4.5}$$

The channel fading is only a function of time t for a flat-flat fading channel, and there is neither time dispersion during the symbol duration T nor frequency dispersion

inside the bandwidth W. The effect of this fading is to multiply a time-variant function to the transmitted signal. So the channel is called a "multiplicative channel."

II. Time-Dispersive Channels:

Time-dispersive channels are dispersive only in time, but not in frequency. The following conditions must hold for this kind of channel:

$$T_M \gg \frac{1}{W} \qquad (T_M \gg T, \text{ dispersive in time})$$

and

$$B_D \ll \frac{1}{T} \qquad (B_D \ll W, \text{ not dispersive in frequency})$$

These channels are also called *frequency-selective fading channels.*

III. Frequency-Dispersive Channels:

Frequency-dispersive channels are dispersive only in frequency, but not in time. The following conditions must be satisfied for these channels.

$$B_D \gg \frac{1}{T} \qquad (B_D \gg W, \text{ dispersive in frequency})$$

and

$$T_M \ll \frac{1}{W} \qquad (T_M \ll T, \text{ not dispersive in time})$$

These channels are also called *time-selective fading channels.*

4.1.2.2 Fading Channel for Indoor Communications

In a typical indoor communication radiotelephone system, the communication is between the base station and a group of portable receivers (users) inside the building. The Doppler spread B_D, which is caused by the motion of the terminals, is very small and typically in the range of 0.3-6.1 Hz[17]. Given the high rate of transmission, the channel can be considered non-dispersive in frequency. Due to reflection, refraction

and scattering of radio waves by structures inside the building, the transmitted signal reaches the receiver through multiple paths. Multipath spread T_M does exist and in many cases $T_M \gg 1/W$. So the indoor communication channel is modeled as a time dispersive, frequency selective channel.

4.1.2.3 Comparison Between MC-CDMA and DS-CDMA

With DS-CDMA, the signal encoding is done in the time domain. Each data bit is transmitted by M time-variant chips. The duration of each chip is $(T_c)_{DS} = \frac{T_b}{M}$. Each chip waveform occupies the whole transmission bandwidth, which is $(W)_{DS} = \frac{M}{T_b}$.

Because the channel is time-dispersive, i.e.,

$$T_M \gg \frac{1}{(W)_{DS}}$$

or

$$T_M \gg (T_c)_{DS} \tag{4.6}$$

Each chip waveform will be dispersed by the channel and the waveform is severely distorted. As we have discussed, the matched filter in the receiver end is to match the waveform of each chip. So it is almost impossible to design the matched filter to match the distortion given the difficulty of modeling the time dispersion of the channel.

One way to deal with this problem is to use the model of multiple resolvable paths with each path representing a different time delay. With large time dispersion, the multiple resolvable paths can be modeled as shown in Figure 4.2 where z^{-1} represents a tap delay of $1/(W)_{DS}$. A RAKE receiver, which has multiple decorrelators each synchronized to a resolvable path, is designed to achieve optimal performance with this model. However, no code exists to ensure that the signals in different resolvable paths are orthogonal. Optimum combining of all resolvable paths with correlated signals from multiple users is a non-trivial problem in DS-CDMA.

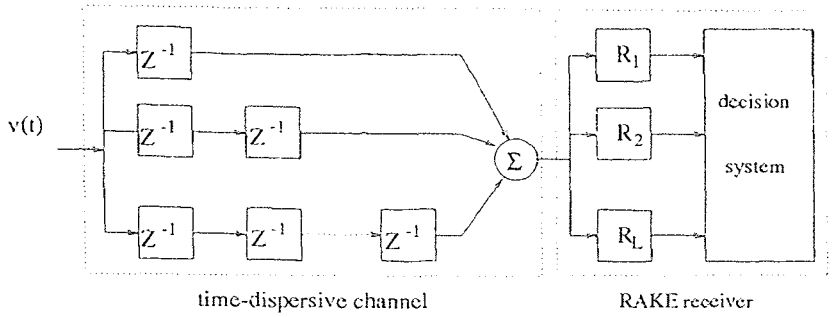

Figure 4.2 Resolvable multipath channel and RAKE receiver

With MC-CDMA, each bit is transmitted as narrowband signals at each subcarrier. These narrowband signals have the symbol duration of $T_{sub} = T_b$ and the bandwidth of $1/T_b$. The total transmission bandwidth is $(W)_{MC} = \frac{MF}{T_b}$. If the time spread T_M can satisfy

$$T_b \gg T_M \gg \frac{T_b}{MF}$$

i.e.,

$$T_{sub} \gg T_M \gg \frac{1}{(W)_{MC}} \tag{4.7}$$

with properly chosen M and F. Even though the channel is frequency selective over the transmission bandwidth ($T_M \gg \frac{1}{(W)_{MC}}$), the signal component at each subcarrier only suffers non-dispersive fading ($T_M \ll T_{sub}$); namely, each narrowband subcarrier signal experiences only narrowband flat-flat fading in an MC-CDMA system.

4.1.2.4 Rayleigh Fading Channel for MC-CDMA

As we have discussed before, the effect of flat-flat fading is to multiply a time-variant function $h(t)$ to the transmitted signal. Due to the stochastic nature of multipath fading, $h(t)$ is modeled as a random process. There are several models for this random process [18]. One well accepted model is Rayleigh fading. This model applies to the indoor communication environment where there is no dominated line-of-sight (LOS) path from the base station to the receiver. In this case, we can assume that the

amplitudes of signal from different paths are approximately the same while the phase delays distributed randomly within $(0, 2\pi)$. At the receiver end, the summation of the signal components from different paths will form a complex Gaussian random process according to the central limit theorem, i.e., $h(t)$ is complex Gaussian. Its amplitude envelope $|h(t)|$ is Rayleigh distributed. The fading which can be modeled this way is categorized as Rayleigh fading[19]. The random process $h(t)$ varies more slowly in time than the transmitted data rate. So for frequency-selective fading channel of MC-CDMA, inside each data symbol duration, the narrowband flat-flat fading at each subcarrier is

$$h_{km} = a_{km} e^{j\theta_{km}} \tag{4.8}$$

where $(_k)$ stands for the channel used by user k and $(_m)$ stands for the m-th subcarrier. a_{km} is the fading amplitude and θ_{km} is the phase shift uniformly distributed on $(-\pi, \pi)$. Subscription $_k$ can be omitted for downlink communication case because all users' signal are transmitted through a common channel. The fading amplitude at each subcarrier m has a Rayleigh distributed probability density function (pdf):

$$f_{a_m}(a_m) = \frac{a_m}{\sigma^2} e^{-\frac{a_m^2}{2\sigma^2}} \tag{4.9}$$

where σ is the Rayleigh parameter.

The cross correlation between fadings at different subcarriers is characterized in [10]

$$\begin{aligned} \gamma_{ij} &= E\{h_i h_j^*\} \\ &= \frac{2\sigma^2(1 + j\frac{2\pi n F T_M}{T_b})}{1 + 4\pi^2 n^2 F^2 T_M^2 / T_b^2} \end{aligned} \tag{4.10}$$

where $n = i - j$.

We can also represent the fading channel in matrix notations. Let $\boldsymbol{h} = [h_1, h_2, \cdots, h_M]^T$, then the cross correlation matrix of this fading vector is

$$\boldsymbol{\Gamma} = E\{\boldsymbol{h}\boldsymbol{h}^\dagger\}$$

$$= \begin{bmatrix} \gamma_{11} & \gamma_{12} & \cdots & \gamma_{1M} \\ \gamma_{21} & \gamma_{22} & \cdots & \gamma_{2M} \\ \vdots & \vdots & \ddots & \vdots \\ \gamma_{M1} & \gamma_{M2} & \cdots & \gamma_{MM} \end{bmatrix} \quad (4.11)$$

where $(^\dagger)$ stands for the Hermitian and γ_{ij} is given in equation (4.10).

4.1.2.5 Effect of Channel on Transmitted Signal

Given the new channel statistics, the transmitted signal of the k-th user after the channel is

$$s_k(t) = b_k(i)\Pi_{T_b}(t - iT_b) \sum_{m=1}^{M} c_k(m)a_m \cos\left[2\pi(f_c + \frac{m-1}{T}F)t + \theta_m\right], \quad (4.12)$$

Figure 4.3 shows the transmitting process considering the channel fading.

At the receiver, we will have the signal from every user as well as additive noise.

$$r(t) = \sum_{k=1}^{K} b_k(i)\Pi_{T_b}(t - iT_b) \sum_{m=1}^{M} c_k(m)a_m \cos\left[2\pi(f_c + \frac{m-1}{T}F)t + \theta_m\right] + n(t) \quad (4.13)$$

where $n(t)$ is the channel's AWGN with a zero mean and a double sided power spectral density of $N_0/2$.

4.1.3 Receiver

The receiver of MC-CDMA consists of a coherent amplitude detector, a signal demultiplexing and an adaptive decorrelating interference canceler.

4.1.3.1 Coherent Detector

The received signal $r(t)$ is first processed by a coherent amplitude detector (see Figure 4.4). We assume that the subcarriers remain orthogonal after transmission over the fading channel. The m-th output of these detectors is:

$$z^m(i) = \frac{2}{T_b}\int_0^{T_b} r(t)\cos[2\pi(f_c + \frac{m-1}{T_b}F)t + \hat{\theta}_m]dt \quad (4.14)$$

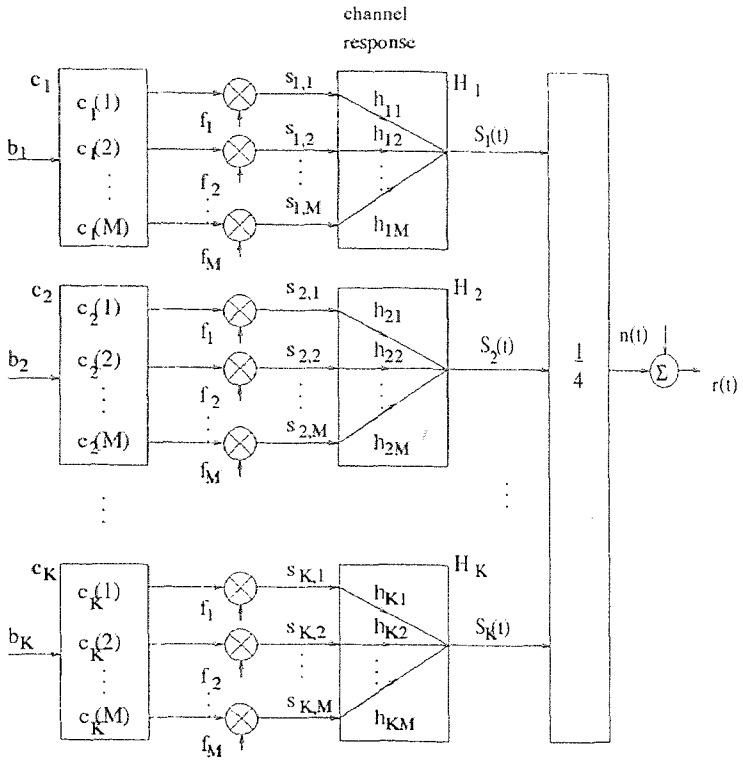

Figure 4.3 Transmitter model and fading channel

where $\hat{\theta}_m$ is the phase of the local oscillator. Assume that perfect phase compensation can be achieved with $\hat{\theta}_m = \theta_m$, along with equation (4.13), we have

$$z^m(i) = \sum_{k=1}^{K} b_k(i)c_k(m)a_{km}\cos(\theta_{km}) + \frac{2}{T}\int_0^T n(t)\cos[2\pi(f_c + \frac{m-1}{T}F)t + \hat{\theta}_m]dt \quad (4.15)$$

4.1.3.2 Demultiplexing

Multiplying the outputs from the coherent detector with the corresponding chips of the signature sequence $\boldsymbol{c}_j$ and summing over the length of the code M, we get the demultiplexed signal for user j as

$$\begin{aligned} x_j(i) &= \sum_{m=1}^{M} z^m c_j(m) \\ &= \sum_{m=1}^{M}\sum_{k=1}^{K} b_k(i)c_k(m)c_j(m)a_{km}\cos(\theta_{km}) + n_j(i) \end{aligned} \quad (4.16)$$

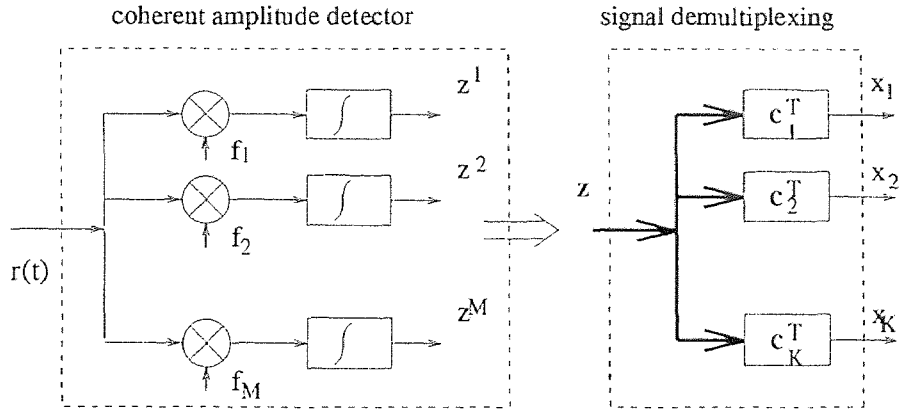

Figure 4.4 Receiver Processor

where

$$n_j(i) = \frac{2}{T}\sum_{m=1}^{M} c_j(m)\int_0^T n(t)\cos 2\pi(f_c + \frac{m-1}{T}F)t \tag{4.17}$$

For the sake of convenience, the index i will be omitted elsewhere in the following sections.

In matrix notations, the output after demultiplexing can be expressed as

$$\begin{aligned} \boldsymbol{x} &= C^T\overline{C}\boldsymbol{b} + \boldsymbol{n} \\ &= \bar{\mathcal{P}}\boldsymbol{b} + \boldsymbol{n} \end{aligned} \tag{4.18}$$

where $\boldsymbol{x} = [x_1, x_2, \cdots, x_K]^T$ and $\boldsymbol{n} = [n_1, n_2, \cdots, n_K]^T$. $\bar{\mathcal{P}}$ is the cross correlation matrix between the code matrix before fading channel C and the code matrix after fading channel $\overline{C}$. Following the same way of defining $\boldsymbol{C}$ in equation (4.4), $\overline{C}$ is defined as

$$\overline{C} = [\overline{\boldsymbol{c}}_1, \overline{\boldsymbol{c}}_2, \cdots, \overline{\boldsymbol{c}}_K] \tag{4.19}$$

where

$$\overline{\boldsymbol{c}}_k = \boldsymbol{A}\boldsymbol{c}_k \tag{4.20}$$

where $\boldsymbol{A}$ is the matrix representation for the channel fading amplitudes; namely, $\boldsymbol{A} = dial(a_1, a_2, \cdots, a_M)$. a_m is the amplitude of h_m defined in equation (4.9). So

we can get the (i,j)-th element in $\bar{\mathcal{P}}$ as

$$\bar{\rho}_{ij} = \sum_{m=1}^{M} c_i(m)c_j(m)a_m \tag{4.21}$$

where $c_i(m)$ and $c_j(m)$ is the m-th chip of the i and j-th user respectively.

4.1.3.3 The Decorrelating Canceler

A decorrelating canceler is used after the demultiplexing for signal separation. The demultiplexed signal vector $\boldsymbol{x}$ is weighted by a weight matrix $\boldsymbol{W}$. Then the weighted interference is subtracted from the desired signal. As is equation (2.22), the output of the canceler of the k-th user is

$$y_k = x_k - \boldsymbol{w}_k^T \boldsymbol{x}_k \tag{4.22}$$

where $\boldsymbol{x}_k$ is obtained from $\boldsymbol{x}$ by deleting x_k, and $\boldsymbol{w}_k$ is the k-th column of the weight matrix $\boldsymbol{W}$ with w_{kk} deleted. $\boldsymbol{W}$ has the same definition as discussed in DS-CDMA.

$$\boldsymbol{W} = \begin{bmatrix} 0 & w_{21} & \cdots & w_{K1} \\ w_{12} & 0 & \cdots & w_{K2} \\ \vdots & \vdots & \ddots & \vdots \\ w_{1K} & w_{2K} & \cdots & 0 \end{bmatrix} \tag{4.23}$$

The weights are obtained adaptively. The control algorithm for weight updating is shown in Figure 4.5.

$$\boldsymbol{w}_k \leftarrow \boldsymbol{w}_k + \mu y_k sgn(\boldsymbol{y}_k) \tag{4.24}$$

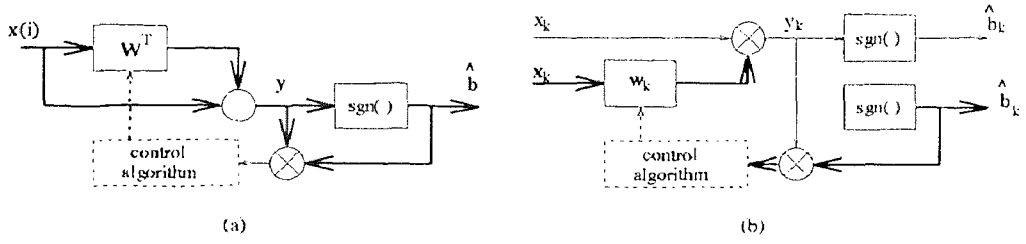

Figure 4.5 (a) Decorrelating canceler (b) k-th branch of the canceler

where $\boldsymbol{y}_k$ is $\boldsymbol{y}$ without the k-th element y_k. Equation (4.24) means that we intend to decorrelate the output of k-th user y_k with other outputs $\boldsymbol{y}_k$; namely, the signal separation is achieved when the outputs are totally decorrelated. Let $\hat{b}_k = sgn(y_k)$, when the function of the decorrelating canceler is achieved, y_k should be uncorrelated with $\hat{b}_j$ of all $j \neq k$ with this updating algorithm. Thus we have

$$E\{y_k \hat{\boldsymbol{b}}_k\} = 0 \tag{4.25}$$

where $\hat{\boldsymbol{b}}_k = [\hat{b}_1, \cdots, \hat{b}_{k-1}, \hat{b}_{k+1}, \cdots, \hat{b}_K]^T$

In most cases, we can assume without loss of generality, that the signal-to-noise ratio (SNR) is large enough so that the major contribution to the error is the multiuser interference. Thus we have,

$$E\{y_k \hat{\boldsymbol{b}}_k\} \simeq E\{y_k \boldsymbol{b}_k\}(1 - 2Pe_k) = 0 \tag{4.26}$$

where Pe_k is the probability of error of the k-th user and $\boldsymbol{b}_k$ is obtained from $\boldsymbol{b}$ by deleting b_k.

4.2 Performance Estimation

4.2.1 Noise Covariance Matrix

Using equation (4.17), we have

$$\begin{aligned} E\{n_j n_i\} &= E\{\sum_{m=1}^{M} c_j(m)\frac{2}{T_b}\int_0^{T_b} n(t)\cos 2\pi(f_c + \frac{m-1}{T_b}F)t dt \cdot \\ &\quad \sum_{n=1}^{M} c_i(n)\frac{2}{T_b}\int_0^{T} n(\xi)\cos 2\pi(f_c + \frac{n-1}{T_b})\xi d\xi \end{aligned}$$

With the assumption that $n(t)$ is white noise with a variance of $\frac{N_0}{2}$; namely

$$E\{n(t)n(\xi)\} = \frac{N_0}{2}\delta(t-\xi)$$

$$
\begin{aligned}
E\{n_j n_i\} &= \frac{4}{T_b^2} E\{\sum_{m=1}^{M} c_j(m) \sum_{n=1}^{M} c_i(n) \frac{N_0}{2} \int_0^{T_b} \cos 2\pi (f_c + \frac{m-1}{T_b} F) \cos 2\pi (f_c + \frac{n-1}{T_b} F) t dt \\
&= \frac{N_0}{T_b} \sum_{m=1}^{M} c_j(m) c_i(m) \\
&= \frac{N_0}{T_b} \rho_{ij} \qquad (4.27)
\end{aligned}
$$

where $\rho_{ij} = \sum_{m=1}^{M} c_j(m) c_i(m)$ for $i \neq j$ and $\rho_{ii} = 1$.

In matrix notation, we have

$$E\{\boldsymbol{n}\boldsymbol{n}^T\} = \frac{N_0}{T_b} \mathcal{P} \qquad (4.28)$$

where $\mathcal{P}$ is the code covariance matrix:

$$(\mathcal{P})_{ij} = \rho_{ij}$$

4.2.2 Local Mean-Received Power

In order to measure the power of the received signal of one particular user, we define the following quantity as the local mean-received power. Accumulated in all subcarriers, the local mean-received power $\bar{p}_j$ is calculated as follows. The signal part of equation (4.16) is

$$x_j = b_j \sum_{m=1}^{M} c_j(m)^2 a_m + \sum_{m=1}^{M} \sum_{\substack{k=1 \\ k \neq j}}^{K} b_k(i) c_k(m) c_j(m) a_m \qquad (4.29)$$

The first term corresponds to user j while the other term is the interfering term. Therefore the local mean-received power of this user $\bar{p}_j$ is:

$$
\begin{aligned}
\bar{p}_j &= E\left\{ \left[\sum_{m=1}^{M} b_j(i) c_j(m)^2 a_m \right]^2 \right\} \\
&= \frac{1}{M^2} E\left\{ \left[\sum_{m=1}^{M} a_m \right]^2 \right\} \\
&= \frac{1}{M^2} E\left\{ \left[\sum_{m=1}^{M} a_m^2 + \sum_{l=1}^{M} \sum_{\substack{n=1 \\ n \neq l}}^{M} a_l a_n \right] \right\} \\
&= \frac{1}{M^2} \left[\sum_{m=1}^{M} E\{a_m^2\} + \sum_{l=1}^{M} \sum_{\substack{n=1 \\ n \neq l}}^{M} E\{a_l a_n\} \right]
\end{aligned}
$$

where $E\{a_m^2\} = 2\sigma^2$ for Rayleigh fading. If the fading at different subcarriers is i.i.d., then $E\{a_l a_n\} = E\{a_l\}E\{a_n\} = \mu^2$, where μ stands for the mean of fading at each subcarrier, and we have $\mu = \sqrt{\frac{\pi}{2}}\sigma$. So $\bar{p}_j$ becomes

$$\bar{p}_j = \frac{2\sigma_j^2}{M}\left[1 + (M-1)\frac{\pi}{4}\right] \tag{4.30}$$

From equation (4.28) the noise power is given as $p_n = \frac{N_0}{T_b}$, so the *local mean-received power to noise ratio* is:

$$LSNR = \frac{2\sigma^2 T_b}{N_0 M}\{[1 + (M-1)\frac{\pi}{4}]\} \tag{4.31}$$

4.3 Simulations

The performance estimation derived in the previous section is conditioned on the fading channel's statistics. It is hard to analyzes, especially when we have dependent fadings on different subcarriers. So, several simulation experiments have been done to evaluate the system performance.

4.3.1 Conditions Applied in the Simulation

There are several conditions to be studied in the simulations: codes, the channel model, and the received signal power.

I. Codes:

Codes chosen as signature sequences should satisfy several requirements for the MC-CDMA communication.

orthogonality: The codes should have a good property against both multi-access interference and self-interference; namely, the cross correlation between codes of different users and the partial auto-correlation of each code should be small.

length: The number of chips in the signature sequence, M, which is also the number of subcarriers in MC-CDMA, can not be too small. Otherwise the argument for equation (4.7) can not hold when we use $F = 1$ to minimize the transmission bandwidth.

In our simulation, we use Gold codes of length $M = 127$. Widely used in mobile communication, Gold Sequence is a pseudo orthogonal code which has excellent correlation properties. For a set of normalized Gold Sequences of length 127, there are only three possible values for the correlation, either cross or auto: $-\frac{1}{127}$, $-\frac{17}{127}$ and $\frac{15}{127}$. If we only pick K out of $M + 2$ possible Gold Codes with $K < M + 2$, we are able to get the cross correlation matrix between these codes, which only has one value: $-\frac{1}{127}$. The codes used by our simulation satisfy this condition.

II. Channel Model:

We use the channel model discussed in section 4.1.2.3. The fading channel is frequency-selective over the transmission bandwidth but flat-flat within the narrowband centered at each subcarrier. As we have discussed before, the effect of flat-flat multipath fading is equivalent to multiplying a time-variant random variable $h_m(t)$ to the signal amplitude with m as the index of the subcarrier. Given the fact that the variation of channel is much slower compared with the symbol rate, it can be reasonably assumed that $h_m(t)$ are fixed with N symbol durations. Those random variables h_m can be modeled either as i.i.d. with Rayleigh distribution or dependent Rayleigh with the covariance matrix given in equation (4.10). $N = 1000$ is used for all the simulations.

III. Received Signal Power and Local SNR:

The received signal power for a particular user is represented by its local mean-received power as defined in equation (4.30). Correspondingly, the local signal-to-

noise ratio ($LSNR$) can be calculated using equation (4.31) for the purpose of making comparison between different simulation schemes.

Notice that when the fadings are dependent at different subcarriers, the local mean-received power can not be obtained from equation (4.30); however, the same $LSNR$ can still be used as a measurement index.

4.3.2 Simulation Results

The idea behind the decorrelating interference cancellation algorithm is to decorrelate the desired signal with interference. By achieving total decorrelation between the receiver outputs, the canceler should be able to cancel the interference adaptively. There are many factors which could affect the adapting process. Two major ones are interference power and the cross correlation between different users' signature sequences. Simulations have been done to show the effect of these two factors. User 1 is taken as the designated user in all the simulations.

4.3.2.1 Effect of the Interference Power

In these simulations, we use Gold codes of length 127 as signature sequences. There are 129 different Gold codes with this length; namely, up to 129 users can be active simultaneously in this MC-CDMA system. In this simulation, we assume the number of active users in the system is 20. As already pointed out in the description of the codes, we will pick a group of codes with the cross correlation between any two different codes of only one value: $-\frac{1}{127}$, thus we can reduce the effect of interference from other users. The error performance is evaluated while changing the power of other users; namely, the power of interference. The results are given in the following two figures. Figure 4.6 shows the error performance versus the $LSNR$ of interference with the $LSNR$ for user 1 fixed to $10dB$, while the $LSNR$ of other users varies from $10 - 20dB$. The channel fading at different subcarriers is modeled as i.i.d.

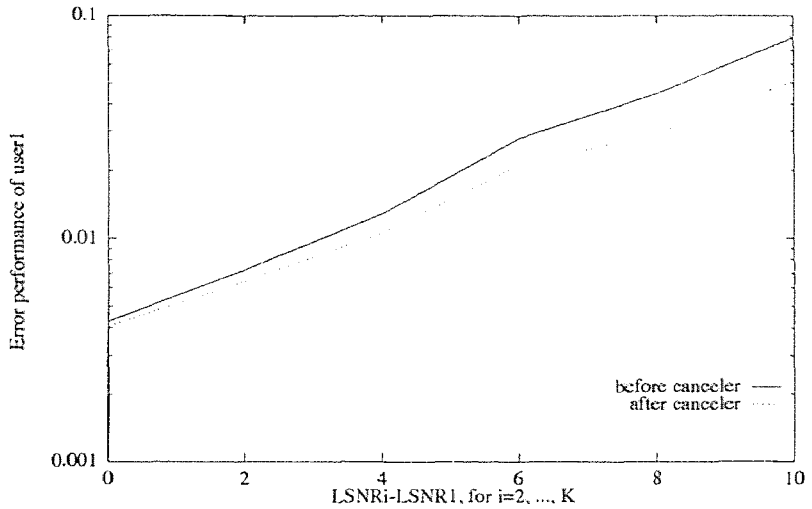

Figure 4.6: Error performance versus interference power (20 users, Gold codes, $LSNR_1 = 10dB$, i.i.d. fading channel)

From this figure we can observe that the improvement made by the canceler increases monotonically with the interference power. This phenomenon can be interpreted as follows. The interference is basically the product of cross correlation and signal power of the users other than the desired user. So when the signal power of other users is small, the overall interference is small. Given this relatively small interference power, the error performance will increase as the consequence. But it will be difficult for the decorrelating canceler to adapt to the optimal weights which can cancel the small interference components from other users. On the other hand, when the signal power from other users becomes large, obviously the overall error will increase. But as having been observed in many experiments, the canceler is more effective when the power of interference is higher. So it is not surprise to see that more improvement show up when the interference is relatively high.

When the channel fadings at different subcarriers are dependent, similar conclusion can be reached as depicted in Figure 4.7. The cross correlations between fadings are given in equation (4.10).

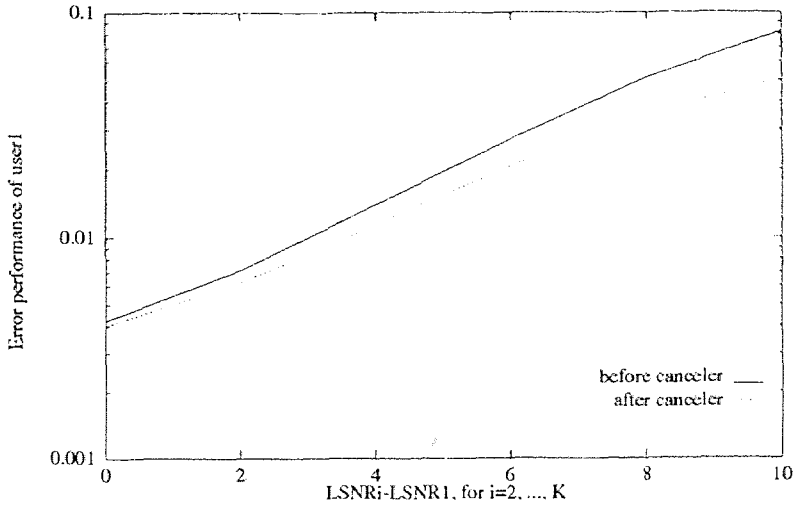

Figure 4.7: Error performance versus interference power (20 users, Gold codes, $LSNR_1 = 10dB$, dependent fading channel)

4.3.2.2 Effect of the Cross Correlations

The cross correlation between codes of the designated user and other users plays an important role in the decorrelating algorithm. Intuitively, if there are some big cross correlation terms which contribute considerably to the interference, somehow the canceler can adapt and cancel those components more effectively than the small terms and thus more significant improvement will occur. In order to prove this point, we repeat the previous simulations with a set of random codes. These codes are generated as binary random sequences of length 127 with their cross correlations randomly distributed in the range of $(0, 1)$. We understand that these random codes are not going to be used in practice. In the cross correlation matrix of these codes, there do exist some relatively larger terms than those of Gold Codes. The results for i.i.d. and dependent channels are shown in Figures 4.8 and 4.9 respectively.

From these figures, we can observe that with bigger cross correlation terms, the interference will increase and the error performance will decrease while the improvement by the canceler becomes more significant. For comparing the performance using these two codes, we combine Figure 4.6 and 4.8 in Figure 4.10. Obviously the

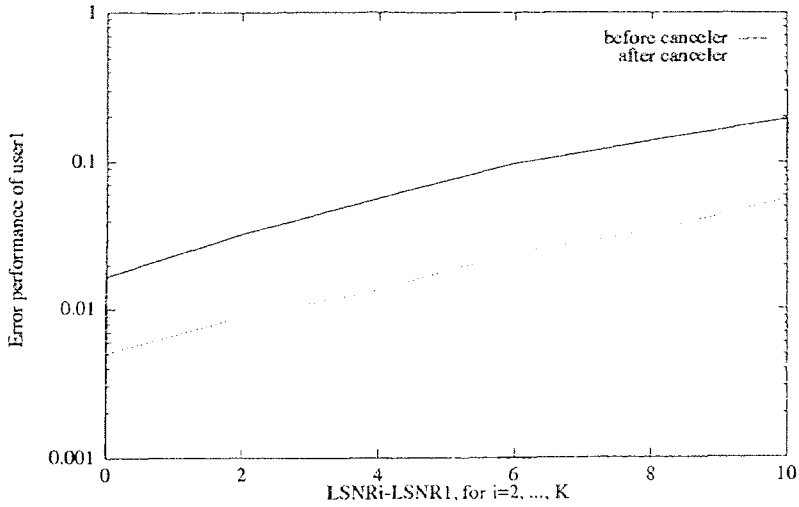

Figure 4.8: Error performance versus interference power (20 users, random codes, $LSNR_1 = 10dB$, i.i.d. fading channel)

canceler works more significant with the random codes. These results are consistent to our theoretical analysis.

4.3.2.3 Error Performance Versus Number of Active Users

We also did the simulations with more active users in the receiver. Using the decorrelating canceler improves the receiver performance for up to 50 users according to the requirement for the practical indoor mobile communication environment.

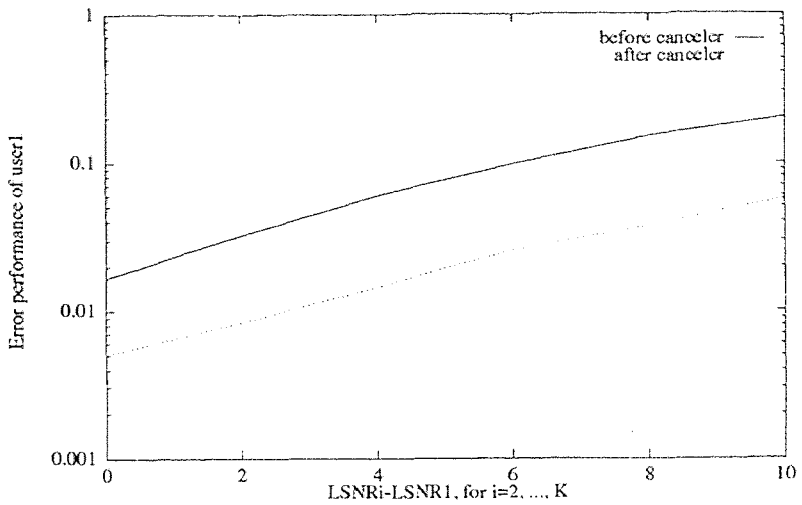

Figure 4.9: Error performance versus interference power (20 users, random codes, $LSNR_1 = 10dB$, dependent fading channel)

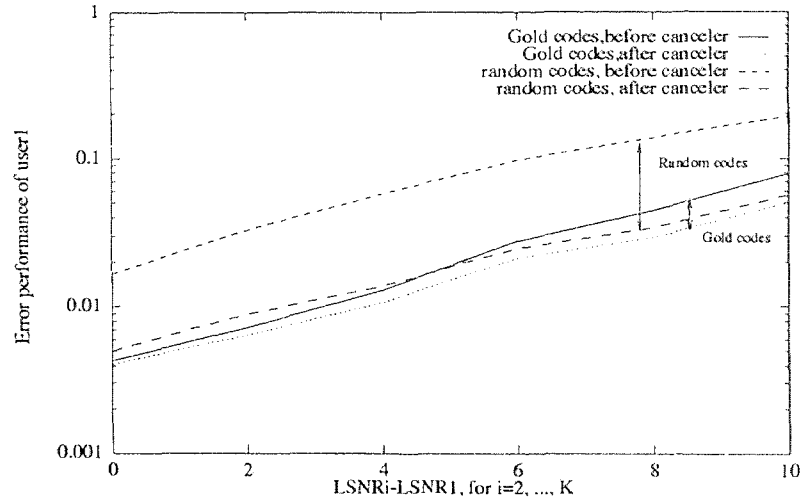

Figure 4.10: Error performance comparison for using Gold codes and random codes (20 users, $LSNR_1 = 10dB$, i.i.d. fading channel)

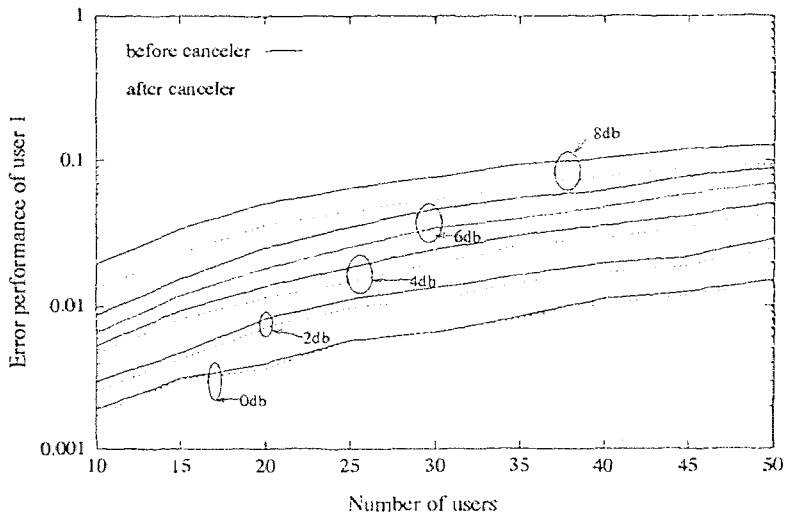

Figure 4.11: Error performance versus number of users with varied interference power(Gold codes, i.i.d. fading channel, $\Delta SNR = 0, 2, 4, 6, 8dB$)

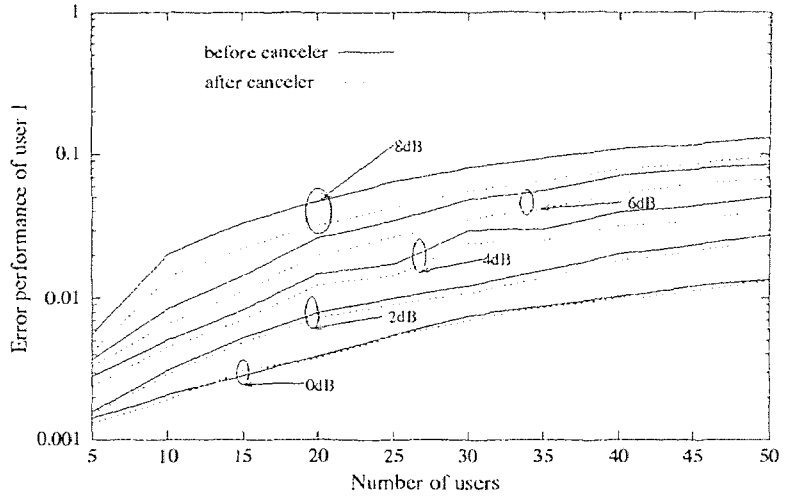

Figure 4.12: Error performance versus number of users with varied interference power (Gold codes, dependent fading channel, $\Delta SNR = 0, 2, 4, 6, 8dB$)

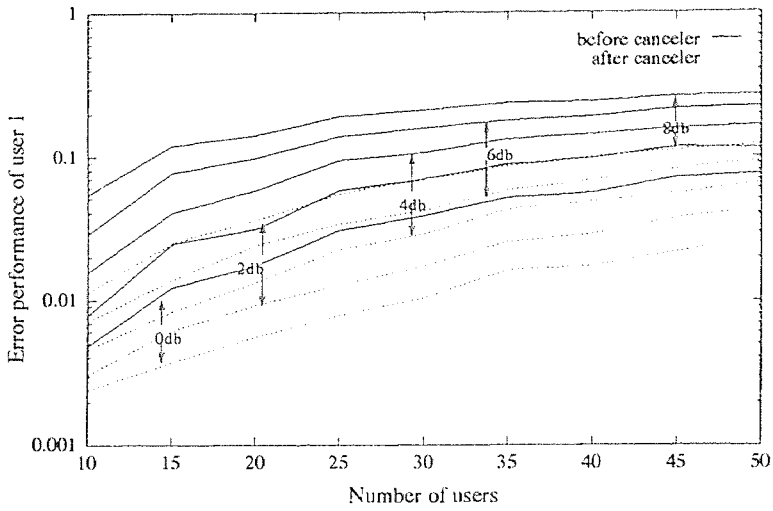

Figure 4.13: Error performance versus number of users with varied interference power (Random codes, i.i.d. fading channel, $\Delta SNR = 0, 2, 4, 6, 8dB$)

CHAPTER 5

CONCLUSION

In this thesis, we have studied several scenarios in which the performance of DS-CDMA receivers can be improved. The system model of MC-CDMA is investigated and the properties of the dispersive multipath channel is incorporated. Several simulation experiments are conducted and the results are consistent with the model proposed. Further work could be done to formulate the fading channel and to find an optimal combination method in the MC-CDMA receiver to optimal and robust signal and interference separation.

APPENDIX A

OPTIMUM WEIGHTS FOR ADAPTIVE RECEIVER USING DEADZONE LIMITERS

A.1 Two User Case

In two user case, the weight matrix and cross correlation matrix are simplied as follows:

$$W = \begin{bmatrix} 0 & w_{12} \\ w_{21} & 0 \end{bmatrix} \tag{A.1}$$

and

$$\mathcal{P} = \begin{bmatrix} 1 & \rho \\ \rho & 1 \end{bmatrix} \tag{A.2}$$

Without loss of generality, we take user 1 as the designated user and calculate the optimum value of $\boldsymbol{w}_1 = w_{21}$. In this case, equation (3.8) becomes

$$E\{y_1 \hat{z}_2\} = E\{(x_1 - w_{21}\hat{z}_2)\hat{z}_2\} = 0 \tag{A.3}$$

Using equation (2.13) and considering the fact that $\hat{z}_2$ is uncorrelated with b_1 and n_1, we have

$$\begin{aligned} E\{y_1 \hat{z}_2\} &= E_{b_2}\{(a_1 b_1 + \rho a_2 b_2 + n_1 - w_{21}\hat{b}_2)\hat{z}_2\} \\ &= E_{b_2}\{\rho a_2 b_2 \hat{z}_2 - w_{21}\hat{z}_2^2\} \end{aligned} \tag{A.4}$$

where E_{b_i} denotes the expected value conditioned on information bit b_i.

In two user case, we consider 2 regions separated by the deadzone threshold:

$$\begin{aligned} D_1 &: \{|z_2| \leq t_{21}\}, \quad \text{inside the deadzone} \\ D_2 &: \{|z_2| > t_{21}\}, \quad \text{outside the deadzone} \end{aligned} \tag{A.5}$$

$E\{y_1 \hat{z}_2\}$ is evaluated in these two parts separately. Using the deadzone property given in equation (3.2), we have

$$E\{y_1 \hat{z}_2\} = E\{y_1 \hat{z}_2, z_2 \in D_1\} + E\{y_1 \hat{z}_2, z_2 \in D_2\}$$

$$
\begin{aligned}
&= E_{b_2}\{\rho a_2 b_2 \hat{z}_2 - w_{21}\hat{z}_2^2,\ z_2 \in D_1\} + E_{b_2}\{\rho a_2 b_2 \hat{z}_2 - w_{21}\hat{z}_2^2,\ z_2 \in D_2\} \\
&= E_{b_2}\{\rho a_2 b_2 \hat{b}_2 - w_{21}, z_2 \in D_2\} \\
&= E_{b_2}\{\rho a_2 b_2 \hat{b}_2 - w_{21}\}\ Pr(z_2 \in D_2) \\
&= \frac{1}{2}\left[E\{\rho a_2 \hat{b}_2 - w_{21}\}\ Pr(|z_2| > t_{21}) + E\{-\rho a_2 \hat{b}_2 - w_{21}\}\ Pr(|z_2| > t_{21})\right] \\
&= (\rho a_2 - w_{21}) Pr(\eta_2 > t_{21} - a_2) + (-\rho a_2 - w_{21}) Pr(\eta_2 > t_{21} + a_2) \\
&= (\rho a_2 - w_{21}) Q\left(\frac{t_{21} - a_2}{\sigma_{\eta_2}}\right) + (-\rho a_2 - w_{21})\left(\frac{t_{21} + a_2}{\sigma_{\eta_2}}\right) \qquad \text{(A.6)}
\end{aligned}
$$

where $Q(\ )$ is the error function. σ_{η_1} and σ_{η_2} are the standard deviations of Gaussian noise η_1 and η_2 respectively. The weight w_{21} can be obtained by equation (A.6) together with (A.3)

$$
w_{21} = \frac{\rho a_2 \left(Q(\frac{t_{21}-a_2}{\sigma_{\eta_2}}) - Q(\frac{t_{21}+a_2}{\sigma_{\eta_2}})\right)}{Q(\frac{t_{21}-a_2}{\sigma_{\eta_2}}) + Q(\frac{t_{21}+a_2}{\sigma_{\eta_2}})} \qquad \text{(A.7)}
$$

Similarly,

$$
w_{12} = \frac{\rho a_1 \left(Q\left(\frac{t_12-a_1}{\sigma_{\eta_1}}\right) - Q\left(\frac{t_12+a_1}{\sigma_{\eta_1}}\right)\right)}{Q\left(\frac{t_12-a_1}{\sigma_{\eta_1}}\right) + Q\left(\frac{t_12+a_1}{\sigma_{\eta_1}}\right)} \qquad \text{(A.8)}
$$

A.2 Three User Case

In three user case, the weight matrix $\boldsymbol{W}$ and the cross correlation matrix $\boldsymbol{\mathcal{P}}$ are 3×3 matrixes. Similarly as the derivation for two user case, we take user 1 as the designated user and calculate $\boldsymbol{w}_1 = [w_{21}, w_{31}]^T$. We divide the (z_2, z_3) space into 4 regions as shown in Figure A.1.

$$
\begin{aligned}
D_1 &: \{|z_2| \le t_{21},\ |z_3| \le t_{31}\} \\
D_2 &: \{|z_2| \le t_{21},\ |z_3| > t_{31}\} \\
D_3 &: \{|z_2| > t_{21},\ |z_3| \le t_{31}\} \\
D_4 &: \{|z_2| > t_{21},\ |z_3| > t_{31}\} \qquad \text{(A.9)}
\end{aligned}
$$

$\boldsymbol{E}\{y_1 \hat{\boldsymbol{z}}_1\}$ is evaluated in these four regions separately. We have

$$
\boldsymbol{E}\{y_1 \hat{\boldsymbol{z}}_1\} = \boldsymbol{E}_1 Pr(\boldsymbol{z}_1 \in D_1) + \boldsymbol{E}_2 Pr(\boldsymbol{z}_1 \in D_2)
$$

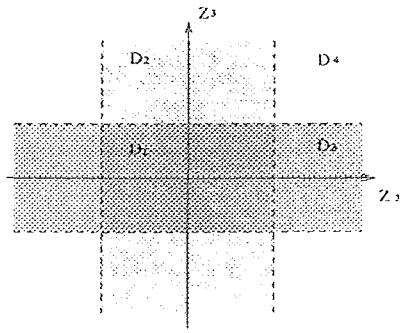

Figure A.1 The 4 sub-regions in 3 user case

$$+\boldsymbol{E}_3 Pr(\boldsymbol{z}_1 \in D_3) + \boldsymbol{E}_4 Pr(\boldsymbol{z}_1 \in D_4) \tag{A.10}$$

with

$$\begin{aligned} \boldsymbol{E}_1 &= \boldsymbol{E}\{y_1 \hat{\boldsymbol{z}}_1 | \hat{\boldsymbol{z}}_1 \in D_1\} \\ &= \mathbf{o} \end{aligned} \tag{A.11}$$

$$\begin{aligned} \boldsymbol{E}_2 &= \boldsymbol{E}\{y_1 \hat{\boldsymbol{z}}_1 | \hat{\boldsymbol{z}}_1 \in D_2\} \\ &= \boldsymbol{E}_{b_2,b_3} \begin{bmatrix} 0 \\ \rho_{13} a_3 b_3 \hat{b}_3 - w_{31} \end{bmatrix} \end{aligned} \tag{A.12}$$

$$\begin{aligned} \boldsymbol{E}_3 &= \boldsymbol{E}\{y_1 \hat{\boldsymbol{z}}_1 | \hat{\boldsymbol{z}}_1 \in D_3\} \\ &= \boldsymbol{E}_{b_2,b_3} \begin{bmatrix} \rho_{12} a_2 b_2 \hat{b}_2 - w_{21} \\ 0 \end{bmatrix} \end{aligned} \tag{A.13}$$

$$\begin{aligned} \boldsymbol{E}_4 &= \boldsymbol{E}\{y_1 \hat{\boldsymbol{z}}_1 | \hat{\boldsymbol{z}}_1 \in D_4\} \\ &= \boldsymbol{E}_{b_2,b_3} \begin{bmatrix} \rho_{12} a_2 b_2 \hat{b}_2 - w_{31} \hat{b}_2 \hat{b}_3 - w_{21} \\ \rho_{13} a_3 b_3 \hat{b}_3 - w_{21} \hat{b}_2 \hat{b}_3 - w_{31} \end{bmatrix} \end{aligned} \tag{A.14}$$

Along with equation (3.8, a linear equation array can be obtained for calculating w_{21} and w_{31}.

$$\begin{cases} M_1 w_{21} + N_1 w_{31} + L_1 = 0 \\ M_2 w_{21} + N_2 w_{31} + L_2 = 0 \end{cases} \tag{A.15}$$

So,

$$\begin{pmatrix} w_{21} \\ w_{31} \end{pmatrix} = \begin{pmatrix} M_1 & N_1 \\ M_2 & N_2 \end{pmatrix}^T \begin{pmatrix} -L_1 \\ -L_2 \end{pmatrix} \tag{A.16}$$

with

$$M_1 = -Q(\frac{t_{21}-a_2}{\sigma_{\eta_2}}) - Q(\frac{t_{21}+a_2}{\sigma_{\eta_2}}) - 2\,(Pr1 + Pr2 + Pr3 + Pr4 + Pr5 + Pr6 + Pr7 + Pr8) \quad \text{(A.17)}$$

$$M_2 = -2(Pr1 + Pr2 + Pr3 + Pr4) + 2(+Pr5 + Pr6 + Pr7 + Pr8) \quad \text{(A.18)}$$

$$N_1 = -2(Pr1 + Pr2 + Pr3 + Pr4) + 2(+Pr5 + Pr6 + Pr7 + Pr8) \quad \text{(A.19)}$$

$$N_2 = Q(\frac{t_{31}-a_3}{\sigma_{\eta_3}}) - Q(\frac{t_{31}+a_3}{\sigma_{\eta_3}}) - 2\,(Pr1 + Pr2 + Pr3 + Pr4 + Pr5 + Pr6 + Pr7 + Pr8) \quad \text{(A.20)}$$

$$L_1 = \rho_{12}a_2\left[Q(\frac{t_{21}-a_2}{\sigma_{\eta_2}}) - Q(\frac{t_{21}+a_2}{\sigma_{\eta_2}}) + 2\,(Pr1 + Pr2 - Pr3 - Pr4 \; Pr5 + Pr6 - Pr7 - Pr8)\right] \quad \text{(A.21)}$$

$$L_2 = \rho_{31}a_3\left[-Q(\frac{t_{31}-a_3}{\sigma_{\eta_3}}) - Q(\frac{t_{31}+a_3}{\sigma_{\eta_3}}) + 2\,(Pr1 - Pr2 + Pr3 - Pr4 \; -Pr5 + Pr6 - Pr7 + Pr8)\right] \quad \text{(A.22)}$$

with

$$Pr1 = Pr(\eta_2 > t_{21} - a_2, \eta_3 > t_{31} - a_3)$$

$$Pr2 = Pr(\eta_2 > t_{21} - a_2, \eta_3 > t_{31} + a_3)$$

$$Pr3 = Pr(\eta_2 > t_{21} + a_2, \eta_3 > t_{31} - a_3)$$

$$Pr4 = Pr(\eta_2 > t_{21} + a_2, \eta_3 > t_{31} + a_3)$$

$$Pr5 = Pr(\eta_2 > t_{21} - a_2, \eta_3 \leq -t_{31} - a_3)$$

$$Pr6 = Pr(\eta_2 > t_{21} - a_2, \eta_3 \leq -t_{31} + a_3)$$

$$Pr7 = Pr(\eta_2 > t_{21} + a_2, \eta_3 \leq -t_{31} - a_3)$$

$$Pr8 = Pr(\eta_2 > t_{21} + a_2, \eta_3 \leq -t_{31} + a_3)$$

APPENDIX B

ERROR PERFORMANCE ANALYSIS FOR RECEIVER USING DEADZONE LIMITERS

B.1 Two User Case

Following the same derivation of equation (3.27), along with the simplified weight matrix $\boldsymbol{W}$ and cross correlation matrix $\boldsymbol{\mathcal{P}}$ given in section A.1, we calculate the error probability of user 1 as follows.

$$
\begin{aligned}
P_{e_1} &= Pr\{\hat{\hat{b}}_1 = 1, b_1 = -1, |z_2| \le t_{21}\} + Pr\{\hat{\hat{b}}_1 = 1, b_1 = -1, |z_2| > t_{21}\} \\
&= \sum_{b_2} [Pr\{-a_1 + \rho a_2 b_2 + n_1 > 0,\ |z_2| \le t_{21}\} \\
&\quad + Pr\{-a_1 + \rho a_2 b_2 - w_{21}\hat{b}_2 + n_1 > 0,\ |z_2| > t_{21}\}] \\
&= \frac{1}{2}[Pr\{-a_1 + \rho a_2 + n_1 > 0\} Pr\{-t_{21} - a_2 \le \eta_2 \le t_{21} - a_2\} \\
&\quad + Pr\{-a_1 - \rho a_2 + n_1 > 0\}\ Pr\{-t_{21} + a_2 \le \eta_2 \le t_{21} + a_2\} \\
&\quad + Pr\{-a_1 + \rho a_2 - w_{21} + n_1 > 0\}\ Pr\{\eta_2 > t_{21} - a_2\} \\
&\quad + Pr\{-a_1 - \rho a_2 - w_{21} + n_1 > 0\}\ Pr\{\eta_2 > t_{21} + a_2\} \\
&\quad + Pr\{-a_1 + \rho a_2 + w_{21} + n_1 > 0\}\ Pr\{\eta_2 < -t_{21} - a_2\} \\
&\quad + Pr\{-a_1 - \rho a_2 + w_{21} + n_1 > 0\}\ Pr\{\eta_2 < -t_{21} + a_2\}] \\
&= \frac{1}{2}\left[Q(\frac{a_1 - \rho a_2}{\sigma_{n_1}}) \int_{-t_{21}-a_2}^{t_{21}-a_2} f_{\eta_2} d\eta_2 + Q(\frac{a_1 + \rho a_2}{\sigma_{n_1}}) \int_{-t_{21}+a_2}^{t_{21}+a_2} f_{\eta_2} d\eta_2 \right. \\
&\quad + Q(\frac{a_1 - \rho a_2 + w_{21}}{\sigma_{n_1}}) \int_{t_{21}-a_2}^{\infty} f_{\eta_2} d\eta_2 + Q(\frac{a_1 + \rho a_2 + w_{21}}{\sigma_{n_1}}) \int_{t_{21}+a_2}^{\infty} f_{\eta_2} d\eta_2 \\
&\quad \left. + Q(\frac{a_1 - \rho a_2 - w_{21}}{\sigma_{n_1}}) \int_{t_{21}+a_2}^{\infty} f_{\eta_2} d\eta_2 + Q(\frac{a_1 + \rho a_2 - w_{21}}{\sigma_{n_1}}) \int_{t_{21}-a_2}^{\infty} f_{\eta_2} d\eta_2 \right] \quad \text{(B.1)}
\end{aligned}
$$

Notice that the above summation has 6 terms. This is consistence with the discussion for equation (3.27).

B.2 Three User Case

Take user 1 as the designated user. The tentative decision region of user 1 is divided into 4 regions D_1, D_2, D_3, and D_4 defined in equation (A.9). Let P_1, P_2, P_3,and P_4 denote the probability of error in each region respectively.

$$\begin{aligned} P_1 &= E_{b_2,b_3} Pr(\hat{\hat{b}}_1 = 1, b_1 = -1, \boldsymbol{z}_1 \in D_1) \\ &= \frac{1}{4}\left[Q\left(\frac{a_1 + \rho_{12}a_2 + \rho_{13}a_3}{\sigma_{n_1}}\right) \int\int_{D_{1_1}} f_{\eta_2,\eta_3}(\eta_2,\eta_3) d\eta_2 d\eta_3 \right. \\ &\quad + Q\left(\frac{a_1 + \rho_{12}a_2 - \rho_{13}a_3}{\sigma_{n_1}}\right) \int\int_{D_{1_2}} f_{\eta_2,\eta_3}(\eta_2,\eta_3) d\eta_2 d\eta_3 \\ &\quad + Q\left(\frac{a_1 - \rho_{12}a_2 + \rho_{13}a_3}{\sigma_{n_1}}\right) \int\int_{D_{1_2}} f_{\eta_2,\eta_3}(\eta_2,\eta_3) d\eta_2 d\eta_3 \\ &\quad \left. + Q\left(\frac{a_1 - \rho_{12}a_2 - \rho_{13}a_3}{\sigma_{N_1}}\right) \int\int_{D_{1_2}} f_{\eta_2,\eta_3}(\eta_2,\eta_3) d\eta_2 d\eta_3 \right] \end{aligned} \tag{B.2}$$

Where $f_{\eta_2,\eta_3}(\eta_2,\eta_3)$ denote the joint *pdf* of correlated Gaussian variables η_2 and η_3. D_{1_1},D_{1_2}, D_{1_3}, and D_{1_4} are the sub-decision regions within D_1 denoted as:

$$D_{1_1} : \{-t_2 - a_2 \le \eta_2 \le t_2 - a_2,\ -t_{31} - a_3 \le \eta_3 \le t_{31} - a_3\}$$

$$D_{1_2} : \{-t_2 - a_2 \le \eta_2 \le t_2 - a_2,\ -t_{31} + a_3 \le \eta_3 \le t_{31} + a_3\}$$

$$D_{1_3} : \{-t_2 + a_2 \le \eta_2 \le t_2 + a_2,\ -t_{31} - a_3 \le \eta_3 \le t_{31} - a_3\}$$

$$D_{1_4} : \{-t_2 + a_2 \le \eta_2 \le t_2 + a_2,\ -t_{31} + a_3 \le \eta_3 \le t_{31} + a_3\}$$

Similarly,

$$\begin{aligned} P_2 &= \frac{1}{4}\left[Q\left(\frac{a_1 + \rho_{12}a_2 + \rho_{13}a_3 - w_{31}}{\sigma_{n_1}}\right) \int\int_{D_{2_1}} f_{\eta_2,\eta_3}(\eta_2,\eta_3) d\eta_2 d\eta_3 \right. \\ &\quad + Q\left(\frac{a_1 + \rho_{12}a_2 + \rho_{13}a_3 + w_{31}}{\sigma_{n_1}}\right) \int\int_{D_{2_2}} f_{\eta_2,\eta_3}(\eta_2,\eta_3) d\eta_2 d\eta_3 \\ &\quad + Q\left(\frac{a_1 + \rho_{12}a_2 - \rho_{13}a_3 - w_{31}}{\sigma_{n_1}}\right) \int\int_{D_{2_3}} f_{\eta_2,\eta_3}(\eta_2,\eta_3) d\eta_2 d\eta_3 \\ &\quad + Q\left(\frac{a_1 + \rho_{12}a_2 - \rho_{13}a_3 + w_{31}}{\sigma_{n_1}}\right) \int\int_{D_{2_4}} f_{\eta_2,\eta_3}(\eta_2,\eta_3) d\eta_2 d\eta_3 \\ &\quad \left. + Q\left(\frac{a_1 - \rho_{12}a_2 + \rho_{13}a_3 - w_{31}}{\sigma_{n_1}}\right) \int\int_{D_{2_5}} f_{\eta_2,\eta_3}(\eta_2,\eta_3) d\eta_2 d\eta_3 \right. \end{aligned}$$

$$+Q\left(\frac{a_1-\rho_{12}a_2+\rho_{13}a_3+w_{31}}{\sigma_{n_1}}\right)\int\int_{D_{2_6}} f_{\eta_2,\eta_3}(\eta_2,\eta_3)d\eta_2 d\eta_3$$
$$+Q\left(\frac{a_1-\rho_{12}a_2-\rho_{13}a_3-w_{31}}{\sigma_{n_1}}\right)\int\int_{D_{2_7}} f_{\eta_2,\eta_3}(\eta_2,\eta_3)d\eta_2 d\eta_3$$
$$+Q\left(\frac{a_1-\rho_{12}a_2-\rho_{13}a_3+w_{31}}{\sigma_{n_1}}\right)\int\int_{D_{2_8}} f_{\eta_2,\eta_3}(\eta_2,\eta_3)d\eta_2 d\eta_3\Bigg] \qquad \text{(B.3)}$$

whit

$$D_{2_1}:\{-t_{21}+a_2\le\eta_2\le t_{21}+a_2,\eta_3<-t_{31}+a_3\}$$
$$D_{2_2}:\{-t_{21}+a_2\le\eta_2\le t_{21}+a_2,\eta_3>t_{31}+a_3\}$$
$$D_{2_3}:\{-t_{21}+a_2\le\eta_2\le t_{21}+a_2,\eta_3<-t_{31}-a_3\}$$
$$D_{2_4}:\{-t_{21}+a_2\le\eta_2\le t_{21}+a_2,\eta_3>t_{31}-a_3\}$$
$$D_{2_5}:\{-t_{21}-a_2\le\eta_2\le t_{21}-a_2,\eta_3<-t_{31}+a_3\}$$
$$D_{2_6}:\{-t_{21}-a_2\le\eta_2\le t_{21}-a_2,\eta_3>t_{31}+a_3\}$$
$$D_{2_7}:\{-t_{21}-a_2\le\eta_2\le t_{21}-a_2,\eta_3<-t_{31}-a_3\}$$
$$D_{2_8}:\{-t_{21}-a_2\le\eta_2\le t_{21}-a_2,\eta_3>t_{31}-a_3\}$$

and

$$\begin{aligned}P_3 = \frac{1}{4}\Bigg[&Q\left(\frac{a_1+\rho_{12}a_2+\rho_{13}a_3-w_{21}}{\sigma_{n_1}}\right)\int\int_{D_{3_1}} f_{\eta_2,\eta_3}(\eta_2,\eta_3)d\eta_2 d\eta_3\\
&+Q\left(\frac{a_1+\rho_{12}a_2+\rho_{13}a_3+w_{31}}{\sigma_{n_1}}\right)\int\int_{D_{3_2}} f_{\eta_2,\eta_3}(\eta_2,\eta_3)d\eta_2 d\eta_3\\
&+Q\left(\frac{a_1+\rho_{12}a_2-\rho_{13}a_3-w_{21}}{\sigma_{n_1}}\right)\int\int_{D_{3_3}} f_{\eta_2,\eta_3}(\eta_2,\eta_3)d\eta_2 d\eta_3\\
&+Q\left(\frac{a_1+\rho_{12}a_2-\rho_{13}a_3+w_{21}}{\sigma_{n_1}}\right)\int\int_{D_{3_4}} f_{\eta_2,\eta_3}(\eta_2,\eta_3)d\eta_2 d\eta_3\\
&+Q\left(\frac{a_1-\rho_{12}a_2+\rho_{13}a_3-w_{21}}{\sigma_{n_1}}\right)\int\int_{D_{3_5}} f_{\eta_2,\eta_3}(\eta_2,\eta_3)d\eta_2 d\eta_3\\
&+Q\left(\frac{a_1-\rho_{12}a_2+\rho_{13}a_3+w_{21}}{\sigma_{n_1}}\right)\int\int_{D_{3_6}} f_{\eta_2,\eta_3}(\eta_2,\eta_3)d\eta_2 d\eta_3\\
&+Q\left(\frac{a_1-\rho_{12}a_2-\rho_{13}a_3-w_{21}}{\sigma_{n_1}}\right)\int\int_{D_{3_7}} f_{\eta_2,\eta_3}(\eta_2,\eta_3)d\eta_2 d\eta_3\\
&+Q\left(\frac{a_1-\rho_{12}a_2-\rho_{13}a_3+w_{21}}{\sigma_{n_1}}\right)\int\int_{D_{3_8}} f_{\eta_2,\eta_3}(\eta_2,\eta_3)d\eta_2 d\eta_3\Bigg] \qquad \text{(B.4)}\end{aligned}$$

with

$$D_{3_1} : \{\eta_2 < -t_{21} + a_2, -t_{31} + a_3 \leq \eta_3 \leq t_{31} + a_3\}$$

$$D_{3_2} : \{\eta_2 > t_{21} + a_2, -t_{31} + a_3 \leq \eta_3 \leq t_{31} + a_3\}$$

$$D_{3_3} : \{\eta_2 < -t_{21} + a_2, -t_{31} - a_3 \leq \eta_3 \leq t_{31} - a_3\}$$

$$D_{3_4} : \{\eta_2 > t_{21} + a_2, -t_{31} - a_3 \leq \eta_3 \leq t_{31} - a_3\}$$

$$D_{3_5} : \{\eta_2 < -t_{21} - a_2, -t_{31} + a_3 \leq \eta_3 \leq t_{31} + a_3\}$$

$$D_{3_6} : \{\eta_2 > t_{21} - a_2, -t_{31} + a_3 \leq \eta_3 \leq t_{31} + a_3\}$$

$$D_{3_7} : \{\eta_2 < -t_{21} - a_2, -t_{31} - a_3 \leq \eta_3 \leq t_{31} - a_3\}$$

$$D_{3_8} : \{\eta_2 > t_{21} - a_2, -t_{31} - a_3 \leq \eta_3 \leq t_{31} - a_3\}$$

and

$$\begin{aligned}
P_4 = \frac{1}{4}\Bigg[& Q\left(\frac{a_1 + \rho_{12}a_2 + \rho_{13}a_3 - w_{21} - w_{31}}{\sigma_{n_1}}\right) \int\int_{D_{4_1}} f_{\eta_2,\eta_3}(\eta_2,\eta_3)d\eta_2 d\eta_3 \\
& + Q\left(\frac{a_1 + \rho_{12}a_2 + \rho_{13}a_3 - w_{21} + w_{31}}{\sigma_{n_1}}\right) \int\int_{D_{4_2}} f_{\eta_2,\eta_3}(\eta_2,\eta_3)d\eta_2 d\eta_3 \\
& + Q\left(\frac{a_1 + \rho_{12}a_2 + \rho_{13}a_3 + w_{21} - w_{31}}{\sigma_{n_1}}\right) \int\int_{D_{4_3}} f_{\eta_2,\eta_3}(\eta_2,\eta_3)d\eta_2 d\eta_3 \\
& + Q\left(\frac{a_1 + \rho_{12}a_2 + \rho_{13}a_3 + w_{21} + w_{31}}{\sigma_{n_1}}\right) \int\int_{D_{4_4}} f_{\eta_2,\eta_3}(\eta_2,\eta_3)d\eta_2 d\eta_3 \\
& + Q\left(\frac{a_1 + \rho_{12}a_2 - \rho_{13}a_3 - w_{21} - w_{31}}{\sigma_{n_1}}\right) \int\int_{D_{4_5}} f_{\eta_2,\eta_3}(\eta_2,\eta_3)d\eta_2 d\eta_3 \\
& + Q\left(\frac{a_1 + \rho_{12}a_2 - \rho_{13}a_3 - w_{21} + w_{31}}{\sigma_{n_1}}\right) \int\int_{D_{4_6}} f_{\eta_2,\eta_3}(\eta_2,\eta_3)d\eta_2 d\eta_3 \\
& + Q\left(\frac{a_1 + \rho_{12}a_2 - \rho_{13}a_3 + w_{21} - w_{31}}{\sigma_{n_1}}\right) \int\int_{D_{4_7}} f_{\eta_2,\eta_3}(\eta_2,\eta_3)d\eta_2 d\eta_3 \\
& + Q\left(\frac{a_1 + \rho_{12}a_2 - \rho_{13}a_3 + w_{21} + w_{31}}{\sigma_{n_1}}\right) \int\int_{D_{4_8}} f_{\eta_2,\eta_3}(\eta_2,\eta_3)d\eta_2 d\eta_3 \\
& + Q\left(\frac{a_1 - \rho_{12}a_2 + \rho_{13}a_3 - w_{21} - w_{31}}{\sigma_{n_1}}\right) \int\int_{D_{4_9}} f_{\eta_2,\eta_3}(\eta_2,\eta_3)d\eta_2 d\eta_3 \\
& + Q\left(\frac{a_1 - \rho_{12}a_2 + \rho_{13}a_3 - w_{21} + w_{31}}{\sigma_{n_1}}\right) \int\int_{D_{4_{10}}} f_{\eta_2,\eta_3}(\eta_2,\eta_3)d\eta_2 d\eta_3
\end{aligned}$$

$$+Q\left(\frac{a_1-\rho_{12}a_2+\rho_{13}a_3+w_{21}-w_{31}}{\sigma_{n_1}}\right)\int\int_{D_{4_{11}}} f_{\eta_2,\eta_3}(\eta_2,\eta_3)d\eta_2 d\eta_3$$

$$+Q\left(\frac{a_1-\rho_{12}a_2+\rho_{13}a_3+w_{21}+w_{31}}{\sigma_{n_1}}\right)\int\int_{D_{4_{12}}} f_{\eta_2,\eta_3}(\eta_2,\eta_3)d\eta_2 d\eta_3$$

$$+Q\left(\frac{a_1-\rho_{12}a_2-\rho_{13}a_3-w_{21}-w_{31}}{\sigma_{n_1}}\right)\int\int_{D_{4_{13}}} f_{\eta_2,\eta_3}(\eta_2,\eta_3)d\eta_2 d\eta_3$$

$$+Q\left(\frac{a_1-\rho_{12}a_2-\rho_{13}a_3-w_{21}+w_{31}}{\sigma_{n_1}}\right)\int\int_{D_{4_{14}}} f_{\eta_2,\eta_3}(\eta_2,\eta_3)d\eta_2 d\eta_3$$

$$+Q\left(\frac{a_1-\rho_{12}a_2-\rho_{13}a_3+w_{21}-w_{31}}{\sigma_{n_1}}\right)\int\int_{D_{4_{15}}} f_{\eta_2,\eta_3}(\eta_2,\eta_3)d\eta_2 d\eta_3$$

$$+Q\left(\frac{a_1-\rho_{12}a_2-\rho_{13}a_3+w_{21}+w_{31}}{\sigma_{n_1}}\right)\int\int_{D_{4_{16}}} f_{\eta_2,\eta_3}(\eta_2,\eta_3)d\eta_2 d\eta_3\Bigg] \quad \text{(B.5)}$$

with

$$D_{4_1}:\{\eta_2<-t_{21}+a_2,\eta_3<-t_{31}+a_3\}$$

$$D_{4_2}:\{\eta_2<-t_{21}+a_2,\eta_3>t_{31}+a_3\}$$

$$D_{4_3}:\{\eta_2>t_{21}+a_2,\eta_3<-t_{31}+a_3\}$$

$$D_{4_4}:\{\eta_2>t_{21}+a_2,\eta_3>t_{31}+a_3\}$$

$$D_{4_5}:\{\eta_2<-t_{21}+a_2,\eta_3<-t_{31}-a_3\}$$

$$D_{4_6}:\{\eta_2<-t_{21}+a_2,\eta_3>t_{31}-a_3\}$$

$$D_{4_7}:\{\eta_2>t_{21}+a_2,\eta_3<-t_{31}-a_3\}$$

$$D_{4_8}:\{\eta_2>t_{21}+a_2,\eta_3>t_{31}-a_3\}$$

$$D_{4_9}:\{\eta_2<-t_{21}-a_2,\eta_3<-t_{31}+a_3\}$$

$$D_{4_{10}}:\{\eta_2<-t_{21}-a_2,\eta_3>t_{31}+a_3\}$$

$$D_{4_{11}}:\{\eta_2>t_{21}-a_2,\eta_3<-t_{31}+a_3\}$$

$$D_{4_{12}}:\{\eta_2>t_{21}-a_2,\eta_3>t_{31}+a_3\}$$

$$D_{4_{13}}:\{\eta_2<-t_{21}-a_2,\eta_3<-t_{31}-a_3\}$$

$$D_{4_{14}}:\{\eta_2<-t_{21}-a_2,\eta_3>t_{31}-a_3\}$$

$$D_{4_{15}} : \{\eta_2 > t21 - a_2, \eta_3 < -t_{31} - a_3\}$$

$$D_{4_{16}} : \{\eta_2 > t_{21} - a_2, \eta_3 > t_{31} - a_3\}$$

REFERENCES

1. S. Verdu, "Minimum Probability of Error for Asynchronous Gaussian Multiple Access Channels," *IEEE Trans. Information Theory*, Vol. IT-32, No. 1, pp. 85-96, Jan. 1986.

2. M. K. Varanasi and B. Aazhang, "Multistage Detector in Asynchronous Code-Division Multiple Access Communications," *IEEE Trans. on Commutations*, vol. 38, No. 4, pp. 509-519, Apr. 1990.

3. M. K. Varanasi and B. Aazhang, "Near-Optimum Detector in Synchronous Code-Division Multiple-Access System," *IEEE Trans. on Communications*, vol. 39, No. 5, pp. 725-736, May 1991.

4. Z. Siveski, Y. Bar-Ness and D. W. Chen, "Adaptive Multiuser Detector for Synchronous Code Division Multiple Access Applications," *1994 International Zurich Seminar on Digital Communications*, Zurich, Switzerland, Mar. 1994.

5. X. Zhang and D. Brady, "Soft-Decision Multistage Detection for Asynchronous AWGN Channels," *31st Annual Allerton Conference on Communication, Control and Computers*, Monticello, IL, Sept. 1993.

6. D.W. Chen, Z. Siveski and Y. Bar-Ness, "Synchronous Multiuser CDMA Detector with Soft Decision Adaptive Canceler," *28th Annual Conference on Information Sciences and Systems*, Princeton, NJ, Mar. 1994.

7. M. Alard and R. Lassalle, "Principles of Modulation and Channel Coding for Digital Broadcasting for Mobile Receivers", *EBU Review-Technical, European Broadcast Union, No. 224*, Aug. 1987, pp. 168-190.

8. S. B. Weinsteis and P. M. Ebert, "Data Transmission By Frequency-Division Multiplexing Using the Discrete Fourier Transform," *IEEE Trans. on Commutations*, Vol. COM-19, pp. 628-634, Oct. 1971.

9. L. J. Cimini, "Analysis and Simulation of a Digital Mobile Channel Using Orthogonal Frequency Division Multiplexing," *IEEE Trans. on Commutations*, Vol. COM-33, pp. 665-675, Jul. 1985.

10. W. C. Jakes, *Microwave Mobile Communications*, Wiley, New York, 1974.

11. N. Yee, J. P. M. G. Linnartz and G. Fettweis, "Multi-Carrier CDMA in Indoor Wireless Radio Networks," *IEEE Personal Indoor and Mobile Radio Communications (PIMRC) Int. Conference*, Yokohama, Japan, Sept. 1993. pp. 109-113.

12. N. Yee and J. P. M. G. Linnartz, "Wiener Filtering of Multi-Carrier CDMA in a Rayleigh Fading Channel," *IEEE Personal Indoor and Mobile Radio Communications (PIMRC) Int. Conference,* The Hague, The Netherlands, Sept. 1994

13. Edward A. Lee and David G. Messerschmitt, *Digital Communication,* Kluwer Academic Press, Boston, 1994.

14. Bin Zhu, "Transient Behavior of an Adaptive Synchronous CDMA Receiver," Master's thesis, Department of ECE, NJIT, Jan. 1994.

15. R. L. Pickholtz, D. L. Schilling and L. B. Milstein, "Theory of Spread-Spectrum Communication - A Tutorial," *IEEE Trans. on Communications,* COM-30, pp. 855-884, May 1982.

16. W. C. Y. Lee, *Mobile Communications Design Fundamentals*, John Wiley & Sons, Inc., New York, 1993.

17. N. Yee and J. P. M. G. Linnartz, "Controlled Equalization for MC-CDMA in Rician Fading Channels," *IEEE Vehicular Technology Conference,* Stockholm, Jun. 1994.

18. Homayoun Hashemi, "The Indoor Radio Propagation Channel," *Proceedings of the IEEE,* Vol. 81, No. 7, Jul. 1993

19. Seymour Stein, "Fading Channel Issues in System Engineering," *IEEE Journal on Selected Areas in Communication,* Vol. SAC-5, No. 2, Feb. 1987.

20. R. Lupas and S. Verdu, "Near-Far Resistance of Multiuser Detectors in Asynchronous Channels," *IEEE Trans. on Communications,* Vol. 38, No. 4, pp. 496-508, Apr. 1990.